University of Alberta

Objective Surgical Skill Evaluation

by

Fraser Anderson

A thesis submitted to the Faculty of Graduate Studies and Research
in partial fulfillment of the requirements for the degree of

Master of Science

Department of Computing Science

©Fraser Anderson
Fall 2010
Edmonton, Alberta

Permission is hereby granted to the University of Alberta Libraries to reproduce single copies of this thesis and to lend or sell such copies for private, scholarly or scientific research purposes only. Where the thesis is converted to, or otherwise made available in digital form, the University of Alberta will advise potential users of the thesis of these terms.

The author reserves all other publication and other rights in association with the copyright in the thesis, and except as herein before provided, neither the thesis nor any substantial portion thereof may be printed or otherwise reproduced in any material form whatever without the author's prior written permission.

Examining Committee

Walter F. Bischof, Computing Science

Pierre Boulanger, Computing Science

Daniel W. Birch, Surgery

Joerg Sander, Computing Science

To Mom and Dad

For teaching me how to read, letting me push buttons, and supporting me for a quarter-century and counting.

Abstract

It is essential for surgeons to have their skill evaluated prior to entering the operating room. Most evaluation methods currently in use are subjective, relying on human judgment to assess trainees. Recently, sensors have been used to track the positions of instruments and the forces applied to them by surgeons, opening up the possibility of automated skill analysis. This thesis presents a newly developed recording system, and novel methods used to automatically analyze surgical skill within the context of laparoscopic procedures. The evaluation methods are tested using an empirical study involving a number of participants with a wide range of surgical skill.

Acknowledgements

Thanks for everything, Michelle. For keeping me on track over the last 2 years, answering the phone in the middle of the night, for being a travel-buddy, and everything else you've done. Thanks for the help with the thesis as well, from looking at all of my wonderful graphs, reading over the thesis, helping with the experiments, building the obviously-too-good-to-be-done-by-me force calibration figure.

Thanks Walter, for going far above and beyond what a supervisor should do. From the 5 minute response times to 2am emails, same day turn around on paper reviews, and the box of red pens you used on my thesis. I apologize for soiling your summer vacation with these drafts. You are an incredible mentor.

Pierre, thank you for all your advice, knowledge, and house parties. You go out of your way to make people feel part of the lab and create a friendly atmosphere.

To Dr. Birch, thanks for the surgical knowledge and interest in the project. Both you and the CAMIS staff were extremely helpful in helping me get set up, getting the ethics approval, finding participants and refining the study. The opportunity to watch live surgical procedures was also incredibly interesting and useful.

Table of Contents

List of Figures

Chapter 1

Introduction

Before surgeons enter the operating room for the first time, it is essential that they have the necessary skills. Without the proper skill set, surgeons can cause severe complications that cost time, patient suffering and death. Prior to performing live surgical procedures, surgeons must undergo a rigorous training and evaluation process to ensure they are competent and able to perform procedures on patients.

Evaluating a surgeon's knowledge can be achieved through written examinations, but evaluating surgical dexterity is more difficult. Current methods of evaluating surgical dexterity are quite subjective, and rely on expert judgment. The expert typically watches a trainee perform a number of surgical maneuvers and assigns the trainee a proficiency score. These scores can vary widely between experts and are thus unreliable. Checklists and scoring sheets, such as the Objective Structured Assessment of Technical Skill rating system (OSATS) [40], are attempts to remove this subjectivity by providing a standardized scoring sheet for surgical tasks. However, this still requires an expert to assess a surgeon's movement, interpret the scoring sheet, and assign a relevant score.

In recent years, technology has been adopted to address the problem of evaluating surgical dexterity [55]. Motion capture and force sensing devices allow a computer to record and analyze the movements made by a surgeon. By relying solely on the data from the sensors, the computer can produce an evaluation of surgical skill that is free from human subjectivity. This method of evaluation has the possibility of being more reliable and accurate than an expert surgeon, but further research is needed.

1.1 Surgical Techniques

Techniques for performing surgery have developed substantially in recent years, providing patients with an unprecedented level of care while introducing new challenges for the surgeon.

Open surgery is the ‘simplest’ surgical technique. This approach involves creating a large incision in the patient through which the surgeon can directly manipulate internal organs. This method is the most traumatic for the patient, as the incision often results in substantial scarring and increased risk of infection. This type of surgery is the least complicated for the surgeon to perform. There is direct access to the tissues, allowing for palpation and the use of the surgeon’s hands and a direct view of the tissue.

Minimally invasive surgery (MIS) is a collection of surgical techniques that offer a reduced-trauma alternative to open surgical procedures. MIS is characterized by its use of unique tools, small incisions, and limited access to the tissues being operated on. Most MIS procedures involve the use of a camera inserted into the patient’s body through a small incision. Long, thin, surgical tools are also inserted into the patient through small incisions. The surgeon views the output of the camera on a video monitor as he manipulates the tissue with various instruments. This approach is more difficult for the surgeon, as there is not direct access to the tissue and the view is through a 2D screen resulting in limited depth perception. Patients benefit from MIS techniques however, as there is less trauma, scarring, and risk of infection with the smaller incisions.

Laparoscopic surgery is a type of MIS in which the camera is part of a rigid instrument called a laparoscope. At the beginning of laparoscopic procedures, the patient is prepared for surgery by creating a number of small incisions in the abdomen that are then filled with trocars. Trocars are small, rubber channels that the camera and instrument are later inserted into. The trocars’ function is to seal the abdomen, as it is inflated with carbon dioxide to lift the abdominal wall off the tissues that are being operated on. The trocars also introduce friction between the surgical instruments and the surgeon’s hands, dampening the haptic feedback from the tool-tissue interactions.

Laparoscopic surgery can be more difficult than open surgery for a number of reasons. The instruments are quite long, causing movements made at the handle to be amplified at the tool tip. The movements are also reversed due to the lever effect of the trocar. Moving the handle to the left moves the tool tip to the right within the surgical field. The operating field is shown on a monitor that is typically placed high above the patient, making it difficult to watch the surgical field and monitor hand position at the same time. The surgical instruments are also limited to five degrees of freedom, thus restricting the movements of the surgeon.

Further developments in surgical technique continue to require more advanced surgical skill. One technique that is gaining momentum is Natural Orifice Translumenal Endoscopic Surgery (NOTES). With this technique, the camera and instruments are embedded in a flexible hose that is inserted through a patient's existing orifices. All incisions are made inside the body, eliminating the scars produced by traditional MIS and open procedures. This approach is quite difficult, as the surgeon has all of the restrictions of existing MIS procedures in addition to the constraints of using a single, fixed point of entry.

Robotic surgery has also gained favour in recent years as an alternative to traditional MIS procedures. This type of surgery is performed with a robotic system, such as the da Vinci system from Intuitive Medical [66]. In this system, the surgeon sits across the room from the patient at a surgical console, and manipulates the robotic arms using a pair of scissor-like devices. These devices currently do not provide haptic feedback or any indication of the amount of force they are applying. The workspace of the devices is also quite small, requiring the surgeon to use a clutching technique to maneuver the instruments. As with other surgical techniques, substantial skill is required to perform operations effectively with the robotic system.

1.2 Skill Evaluation

Accurate evaluation of surgical skill is necessary to ensure surgeons have adequate skills to operate on live patients. As part of the training process, an evaluation informs trainees of what skills they need to improve on. Periodic evaluations can be useful to surgeons throughout their careers as well. Evaluation can also be used in research, to examine what factors affect surgical proficiency. The effect of drugs, lack of sleep, stress, or time away from the operating room (OR) can all benefit from a reliable metric for surgical skill.

As surgeons get older and their surgical skills can decrease [6, 74], and they should be re-certified periodically through an evaluation to ensure they are still capable of performing the necessary tasks. This re-certification would involve a test of both psychomotor skills and cognitive ability. An automated, objective evaluation would be ideal for this scenario, as it would eliminate any bias that would come from a peer evaluation among experts.

1.2.1 Subjective Surgical Skill Evaluation

Current methods for evaluating surgical skill are still largely subjective. Some efforts have been made, such as the development of the OSATS rating system that attempt to standardize evaluation, but these still involve subjective expert evaluation. With this system, an expert must assign scores, e.g., using a Likert scale from 1 to 5, in areas such as ‘respect for tissue’, ‘time and motion’, and ‘knowledge of instruments’. Each of these areas has associated anchors, for example, a student would score 1 if they ‘frequently used unnecessary force on tissue or caused damage by inappropriate use of instruments’, 3 if they performed ’careful handling of tissue but occasionally caused inadvertent damage’, and 5 if they ‘consistently handled tissues appropriately with minimal damage’. This scale still leaves much room for the expert to interpret what is meant by ‘unnecessary force’, and what constitutes ‘frequent’ or ‘occasional’. The lack of clear definitions can lead to large variation in the scores assigned by different experts.

The Global Operative Assessment of Laparoscopic Skills (GOALS) [71] is a similar scoring system that consists of three rating criteria. The first are a number of rating scales that have an expert assessing the psychomotor skills of the participant, such as depth perception, bimanual dexterity, etc. There is also a checklist component to assess aspects of certain operations. Finally, there are two scales for the expert to rate task difficulty, and overall perceived competency. This measuring device is quite useful and reliable in assessing skill, but it requires an evaluator to provide feedback, and there are a number of items requiring subjective analysis.

The Fundamental Laparoscopic Skills (FLS) program [21] includes a set of standardized training and evaluation tasks that can be used to assess a novice's laparoscopic dexterity. These tasks include a pegboard drill, a suturing task, and a cutting task. For the cutting task, the measures are purely objective taking into account only the time to completion and the deviation from the ideal path. Other tasks, such as the suturing task require subjective opinion to assess knot quality. Evaluation using this system also gives very poor feedback to the participants by way of what they could do to improve their skills.

1.2.2 Automated Objective Surgical Skill Evaluation

Automated analysis of surgical movements by computers has the potential to assess surgical skill without any human subjectivity. With this approach, the movements of the surgeon are digitized using special equipment and processed on a computer.

This type of evaluation is not yet widely used, as there are still a number of issues with its implementation. Foremost is the use of specialized recording equipment. This equipment is often expensive and difficult to construct. Some approaches use custom fabricated mechanical systems that attach directly to surgical instruments making it difficult to switch instruments and restricting the movements allowed by the surgeon. Other systems track the surgical instruments using optical or electromagnetic motion capture systems, but these systems often place restrictions on the environment they can be used in. In all cases, additional equipment must be added to the laparoscopic instruments, restricting their use to research environments and virtual reality (VR) trainers.

Another issue preventing widespread adoption of automated evaluation is the lack of clear, reliable metrics for surgical skill. Most research in the area of surgical skill evaluation area focuses on the development and testing of measures that may correlate with surgical skill. Some of these measures are simple measures that quantify the amount of instrument motion, or the length of time taken to complete the task. These measures can be reliably used to distinguish between experts and novices, but they provide only very coarse measures of skill and do not speak to the quality of the movements. Measures that do assess movement quality, such as motion smoothness or peak force tend to be less reliable when used to distinguish amongst skill levels, though they may provide more useful feedback to trainees.

More complex analyses have been performed on the recorded movements at a local level. These approaches use mathematical tools such as Hidden Markov Models to represent and compare gestures. This local analysis has the benefit of being able to provide feedback on the various stages of the task being performed, as well as providing feedback on the quality of the movements. With this method, a model must be extensively trained by expert surgeons on the system that is being used to test on, so it is not possible to transfer models between systems and create one reference 'expert model' that can be widely used.

Experiments in the area of surgical skill evaluation take place in a number of environments. Some studies have taken place in the operating room, getting valuable data from experts performing live surgeries. Others take place in a laboratory or classroom setting, using synthetic tissue or virtual reality trainers. The classroom setting is where most training and evaluation will take place. It is important that students are able to get feedback in this environment, and that they can be assessed before entering an OR. The studies in the OR are essential as well, as the surgical skill metrics must not only apply to the skills demonstrated in classroom tasks, but they must predict performance in the OR as well.

1.3 Contributions and Organization

1.3.1 Contributions

This thesis provides several contributions to the field of surgical skill evaluation. First, a novel system design is presented. This system is capable of recording the position and orientation of laparoscopic instruments as well as the force and torque applied to them. All measurements are synchronized and stored for offline processing. The system was implemented and used in an empirical evaluation, demonstrating its effectiveness.

The empirical user study includes several novel elements. The data set recorded is very rich including two video streams, the movements of the instruments, the forces and torques applied to the laparoscopic instruments, the kinematics of each participant's upper body, and an audio recording of each trial. The participant pool was diverse as well, including at least one participant from each of the five years of surgical residency, surgical fellows, and expert surgeons. While only a subset of the data was analyzed in this thesis (instrument position and forces), the rest of the data will be analyzed in the future to determine what information can be obtained from the surgeon's upper body kinematics and the tool orientation.

Two novel global measures are presented, and their relation to surgical skill is evaluated. Total energy used in manipulating the surgical instrument is computed from the data and is found to correlate with surgical skill for many tasks. Mean and peak energy are also computed, but they do not appear to relate to surgical skill. A number of previously investigated measures are also computed from the data and compared. The usefulness of some of these measures, such as motion smoothness and force features have been debated in the literature, and we find that they do not correlate with surgical skill.

Two novel methods of local analysis are proposed, as well as the use of consistency as an indicator of surgical skill. The analyses are based on the curvature of the trajectory in 3D space, and the energy that is applied during the execution of the tasks. While neither of the analyses demonstrates a clear differentiation between expert and novice, they do show promise, and further research may show them to be valuable. This analysis is unique in that it does not reduce each gesture to a single number, but compares the trajectories and energy signals of entire gestures to one another. This type of analysis is essential to creating a system that is able to give valuable feedback to trainees.

1.3.2 Thesis Organization

Chapter 2 introduces the existing research in the field of surgical evaluation. The systems that are used to record the surgical movements, the measures used to evaluate the participants, and the environments that the experiments are performed in are detailed. Particular attention is paid to laparoscopic surgical evaluation, but relevant work that has been conducted within general surgery and robotic surgery is included as well. Chapter 3 describes the system that was designed and implemented. The hardware and software used to capture the data, as well as the algorithms used to filter and process the data are presented. The experimental procedure used in the empirical study is presented in Chapter 4. The analysis of the data and the discussion of the results are provided in Chapter 5.

Chapter 2

Objective Evaluation of Surgical Skill

The effectiveness of automatic evaluation of surgical dexterity is contingent upon three factors, the technology used to capture the movements of the surgeon, the analysis methods used on the collected data, and the types of tasks that the surgeon performs. This review covers the state of the art in each of these areas while focussing on laparoscopic surgery.

2.1 Experimental Methods

Measures of laparoscopic skill should reflect a surgeon's performance in the operating room while operating on live humans. The recording of objective measures in this environment is difficult due to stringent requirements on the equipment and the more uncontrolled, variable tasks performed. While some researchers have studied skill metrics in the OR, many use artificial training environments such as virtual reality or tasks on synthetic tissue [16, 44]. It is essential that the metrics used to evaluate skill in the artificial training environments reflect the OR performance as much as possible, as they will be used to verify that new surgeons are competent enough to operate on patients.

2.1.1 Experiments In Vivo

In Vivo experiments on both animals and humans have been performed with systems that record kinematic (motion) and dynamic (force) data from the surgeon.

These experiments capture many factors that are impossible to simulate accurately outside the OR, such as the stress of working with a human life, true haptic feedback, and complex visual scenes with various fluids and smoke occluding the anatomy. These experiments are also the most difficult to standardize and control, as there are substantial variations in patient anatomy, differences in OR configuration, and small errors that can result in substantial complications.

Surgery on animals provides researchers with an environment that is almost identical to surgical procedures on humans. Pigs are often used as they are anatomically very similar to humans. The same operations, such as a laparoscopic cholecystectomy or Nissen fundoplication, can be performed on pigs in much the same way that they are performed on humans [56]. These operations are nearly identical to human operations in terms of the equipment used, the tissue mechanics, the presence of fluid and smoke in the visual field, and the presence of possible complications. What these operations lack is the surgeon's knowledge that a human life is at stake, which can cause stress, resulting in errors, tremors and hesitation. To better regulate the variation when using in vivo models, larger procedures have been decomposed into smaller, more controlled segments such as: running the bowel right to left, dissecting mesenteric arteries, passing a suture, tying a knot, and passing stomach behind the esophagus [58, 9]. Although the use of pig models has fewer ethical concerns than operations on humans, the operations are fairly costly and time consuming to prepare, and hence studies tend to have few experiments, usually under ten.

To ensure that the skill evaluations are relevant, the skill measures must be tested in surgical operations on a human where all relevant factors are present. These experiments are often very similar to the experiments with animal models. For example, Hwang et al. [31] had four surgeons perform a laparoscopic cholecystectomy on human patients. The study found that some of the measures that indicate skill, such as mean velocity and acceleration do in fact transfer to operating rooms, but the size of the study was too small to reach conclusions about all measures analyzed. A subsequent study involving six participants, more complex modelling, and task decomposition showed a clear difference between novices and experts in the kinematics of their dominant hand, but not their non-dominant hand [18].

2.1.2 Experiments with Synthetic Trainers

Synthetic trainers offer a highly controlled, somewhat realistic environment that can be easily used in a laboratory environment. Synthetic trainers can take many forms, including box trainers, such as the Endo-trainer, or Virtual Reality trainers, such as the LapMentor [1, 67]. Each of these trainers offers both dexterity tasks and tissue simulation, providing several testbeds to evaluate surgical skill. In order for objective evaluation to be useful, it is essential that skill can be judged from tasks on synthetic tissue. Surgeons will use these synthetic tasks to demonstrate their competency before performing operations on real patients.

Experiments with Synthetic Tissue

Synthetic tissue comes in various forms, e.g., bowels, arteries or skin pads. It mimics the properties of real tissue and provides highly realistic haptic and visual feedback. It is used extensively in surgical training because it is cheap, risk free, and allows surgeons to learn and practice their skills at their own convenience. For the training of laparoscopic operations, the synthetic tissue is typically placed inside a box trainer and manipulated with real laparoscopic instruments. Suturing is the most common operation performed with synthetic tissue, but the tissue can also be cut and manipulated to simulate more complex tasks. While suturing is not an extremely common operation in the operating room, as surgeons often use staples to close wounds, it is still very useful to analyze surgical skill. It challenges the manual dexterity of the surgeon, as manipulating the needle and thread require substantial dexterity with the laparoscopic instruments. It is also cognitively challenging, as the surgeon has to plan his movements carefully, think about the type of knot used, and the movements required to complete the task.

Within the context of laparoscopic skill evaluation, synthetic skin offers a method to conduct controlled, repeatable experiments so that measurements can be more easily compared within groups. Each participant performs the same tasks on the same tissue with the same instruments, eliminating many of the variations that occur with in vivo operations, such as anatomical variations, complications and varying procedures. The low cost and high availability of synthetic tissues make it practical to have studies with large numbers of participants, often more than 50 [19].

Various types of sutures on synthetic tissue have been used in research [69, 25]. Bann et al. had participants perform four types of sutures on a synthetic skin pad using open surgery techniques [4]. The suture types (e.g., simple interrupted, vertical mattress, continuous running, and figure of eight) represent tasks of varying difficulty. On all tasks, entry and exit points were marked on the tissue to provide greater standardization between participants. Estimating skill from various measures was more successful with the more difficult suturing tasks.

Experiments with non-Surgical Dexterity Tasks

Non-surgical tasks have also been used to predict laparoscopic proficiency. These include standardized tasks, such as the FLS McGill Inanimate System for Training and Evaluation of Laparoscopic Skills (MISTELS) [21] as well as ad-hoc tasks requiring laparoscopic dexterity. The FLS MISTELS consist of a set of simple tasks with standardized benchmarks to evaluate laparoscopic dexterity. The most popular task within this set is the pegboard task which requires participants to transfer collars from peg to peg through a laparoscopic interface. An evaluator records the task time and the number of collars dropped. These measures are then used to compute a proficiency score. By recording the kinematics of participants as they performed the pegboard task, Ritter et al. were able to correlate motion-based measurements with the standard FLS proficiency score [57].

A variety of ad-hoc tasks have been used to evaluate laparoscopic dexterity, such as the balls, ring, and elastic band tasks used by Chmarra et al. [15]. Carefully crafted tasks allow researchers to examine very specific movements or exercise specific skills, but they are often not representative of real operating room actions. To study a surgeon's use of the laparoscopic camera, Chmarra devised a task that required participants to touch a number of cylinders spread out inside a training box using laparoscopic instruments [16]. Standardized tests could not be used in this study, as they can be completed without manipulating the camera at all.

Virtual Reality Simulators

In recent years, Virtual Reality (VR) simulators have gained popularity as alternatives to traditional training on synthetic tissue or animal models. These trainers usually consist of simulated laparoscopic instruments with various sensors, actuators, and a 2D display that simulates the view from a laparoscopic camera. Users can practice entire virtual operations or perform a number of practice drills aimed at improving specific techniques. The sensors and actuators on the instruments provide force feedback and an immersive experience. Simulators provide a simple method to gather and analyze movement data, as the devices are fitted with sensors that allow the simulator to track position and orientation of the instruments. The computer-driven graphics also allow the experimenter to precisely control the tasks, permitting greater repeatability and consistency in the experiments.

Both full operations as well as simple dexterity tasks are supported with the software provided with most VR systems. The convenient and affordable nature of these systems makes it possible to use large numbers of subjects, with some studies reporting over 150 [50]. Other studies have made use of the virtual camera interface and have had participants manoeuver the camera inside of a virtual abdomen, allowing researchers to analyze camera movement in a more realistic environment [44]. The majority of reports using VR systems have not used full operation simulations, but used only simple dexterity tasks [70, 72, 68].

2.2 Recording Systems

Several systems have been developed to capture the movements of a surgeon's tools (kinematics) and the forces and torques that are applied to them (dynamics). Each system is unique in the accuracy of the data that it captures, the range of motions it allows, its suitability for different environments, and many other factors. Within each system, the underlying technologies have a substantial influence on these factors and provide a convenient categorization to analyze the systems. Systems that completely record the movement of laparoscopic instruments must be able to measure five degrees of freedom: opening and closing of the handle, translation along the shaft, and rotation around the insertion point in all three dimensions. A review of a number of recording systems can be found in Chmarra et al. [14] which focusses primarily on mechanical motion capture systems.

2.2.1 Electromagnetic Motion Capture

Electromagnetic (EM) tracking systems consist of a device that emits an electromagnetic field and a set of sensors whose position and orientation is recorded within that electromagnetic field. In contrast to optical tracking systems, these systems are robust to occlusions, resulting in a continuous stream of data. The sensors are quite small, hence they can be attached to a variety of existing surgical tools. These systems are, however, quite cumbersome to use because each of the sensors is attached to the recording unit by long wires and the emitter must be quite close to the sensors. The magnetic field is also heavily distorted by metallic objects, resulting in noisy and distorted measurements in a clinical environment.

EM tracking was used in one of the first systems designed for skill evaluation, the Imperial College Surgical Assessment Device (ICSAD) (Figure 2.1) [20]. The ICSAD used the Polhemus Isotrak II tracking system and required a sensor placed on the back of each hand to track the movements of surgeons performing open surgery tasks [4, 19, 64], but has since been adapted to laparoscopic procedures [75, 23]. The ICSAD system captures position information at a rate of 20Hz, a resolution of 1mm and does not use orientation information.

Feng et al. describe a tracking system that uses the MicroBIRD sensors from Ascension Technology to track laparoscopic instruments [28]. These sensors capture the position and orientation of the tip of the instrument within 1.4 mm and 0.5 degrees respectively. While this system was only used in laboratory testing, Dubois et al. describe an EM-based system capable of being deployed in an OR [24]. The position and orientation of the instrument were tracked to an accuracy of 1.8 mm and 0.5 degrees. In their experiments with pig models, Dubois et al. constructed a custom operating table made out of PVC. While this table eliminated a large source of magnetic interference, the use of PVC made it impractical for deployment in operations on humans. Both Feng et al. and Dubois et al.'s systems had a tracking

Figure 2.1: ICSAD system used in the evaluation of open surgical skills [20].

volume of less than one cubic meter. A small number of studies have used EM tracking systems in the OR with humans, but no details were presented with respect to the accuracy of the systems [18, 29].

2.2.2 Optical Motion Capture

Optical motion capture systems can track objects in 3D space by locating markers in video streams. Most optical motion capture systems, such as the MotionAnalysis [2] or Vicon [73] systems, track objects using a number of cameras in conjunction with reflective passive markers placed on the objects. Other systems, such as the OptoTrak [46] and the VisualEyez [51] use active markers, (i.e. infrared LEDs) to locate the objects. Systems using active markers require wires to power the markers. This can impact the movements of the tracked subject, but these systems are often more accurate than their passive counterparts. Optical tracking systems differ with respect to frame rates, accuracies and physical constraints, but all require a line of sight between the camera and markers. This susceptibility to occlusion makes it difficult to use optical tracking systems in operating settings because the tool tip is occluded by the body and operating rooms are often crowded with people and equipment.

Emam et al. used a set of reflective markers placed on the upper body (Figure 2.2) to monitor the motions of the shoulders and elbows of novices and experts [26]. Their system was accurate to 2 mm, but was too bulky to be used in an operating environment. The same system was also used in other studies that analyzed ergonomic factors in laparoscopy [27].

Optical tracking can be combined with electromagnetic tracking to add redundancy and improve the quality of data, as in Hwang et al.'s study [31]. In this system, sensors were placed on a single laparoscopic grasper, which was used in a number of laparoscopic cholecystectomy operations on human subjects. While data on the accuracy in the operating room setting was not provided, the data was accurate enough to distinguish between novices and experts using a number of measures.

Figure 2.2: Upper body motion capture system from Emam et al. [26]

The ProMIS simulator from Haptica [50] is a training system that uses the video stream from a laparoscopic camera to locate the position of markers placed on the tip on the surgical instrument. Although this approach cannot be used in a surgical environment in its current form, the use of the laparoscopic camera view to track tool positions has great potential. No additional equipment would be needed and the surgeon's movements could be monitored during all operations. The availability and ease of use of the ProMIS system has led to numerous studies [57, 44].

2.2.3 Mechanical Motion Capture

Surgical motions can also be tracked using instrumented mechanical links attached directly to surgical tools. The joints of the mechanical links are fitted with angle encoders, usually rotational potentiometers or optical encoders. From these joint angles, the system can accurately reconstruct the position and orientation of the attached instrument using forward kinematics. Usually, the tools are placed inside a gimbal mechanism to provide extra degrees of freedom. A fairly comprehensive review of the various mechanical motion capture devices used in both research and commercial applications can be found in Chmarra et al. [14].

Mechanical motion capture devices most commonly appear as part of a virtual reality training package, such as the LapSim (Figure 2.3) or LapMentor (Figure 2.4a) [35]. The workspace for these virtual trainers is inherently small, instruments do not need to be interchanged, and the mechanical linkages allow for force feedback to the user. This type of tracking has low noise, very little drift, and is not affected by the presence of metallic objects. The TrEndo system [13] uses the sensors from optical computer mice to sense four degrees of freedom (all but the opening and closing of the handle) of a laparoscopic instrument. While not suitable for use in the OR, the accuracy of 0.06 mm in position and 1.27 degrees in rotation make these devices suitable for recording surgical movements on synthetic tissue and virtual trainers with a high degree of precision [15, 16].

The bulky and cumbersome nature of these systems makes them difficult to use in an operating environment. To date, no systems with mechanical motion capture have been used in operations on humans, but the Blue DRAGON system by Rosen et al. (Figure 2.4b) was used to record movements during laparoscopic operations on animal models [58]. The Blue DRAGON is composed of a laparoscopic instrument mounted on a standard four-bar mechanism. Each joint in the four-bar mechanism are fitted with potentiometers to locate the tooltip and a linear potentiometer in the handle to measure the grasping angle. The successor of the Blue DRAGON, the Red DRAGON, uses a spherical mechanism instead of the four-bar linkages used in the Blue DRAGON, making it more compact and portable [30]. Both systems are able to record all five degrees of freedom at 30Hz.

Figure 2.3: LapSim system from Surgical Science [35]

(a) LapMentor system from Simbionix [67].

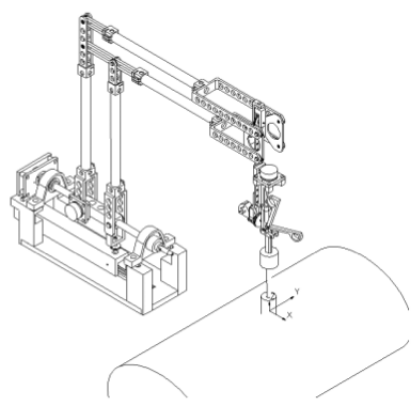

(b) CAD drawing of the Blue DRAGON system from Rosen et al. [58].

Figure 2.4: Systems employing mechanical motion capture for instrument tracking.

2.2.4 Force Transducers

Regardless of the mechanism used to capture the instrument's motion, all systems that record forces and torques do so using strain gauges. Strain gauges are small electronic sensors that modify their voltage output based on the mechanical strain. By combining and calibrating several strain gauges, one can build a sensor capable of measuring the forces and torques applied to them in multiple axes. Most commonly, force and torque sensors are mounted on the shaft of the laparoscopic instrument (Figure 2.5) to capture the dynamics between the surgeon's hand and the tool tip [24, 31, 34, 56, 30]. The majority of these sensors are 6 DOF force/torque sensors from ATI Industrial [3]. The use of these sensors requires irreversibly modifying the laparoscopic instruments, thus preventing their widespread use. Sensors in this configuration are able to record forces in a range of approximately $\pm$ 20 N and torques in a range of $\pm$ 1 Nmm.

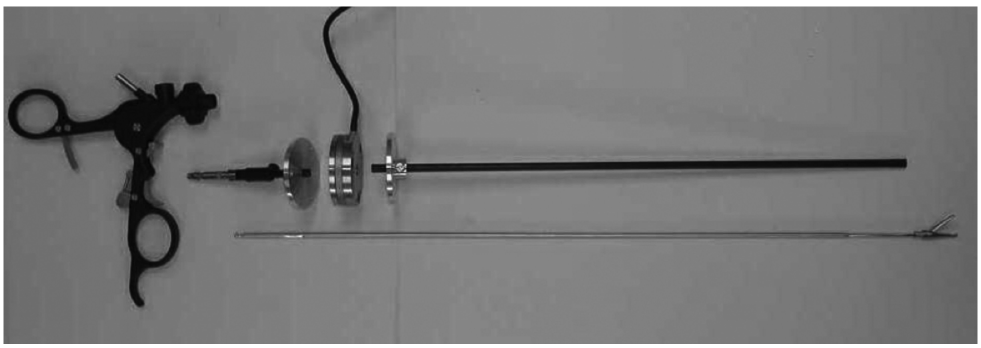

Figure 2.5: Components of force sensor mounted inline with instrument shaft, from Lamata et al. [34].

In other approaches, force and torque sensors are placed underneath the tissue that is being operated on [25]. This configuration is easier to construct as the laparoscopic instruments do not need to be modified. Such a configuration is, however, impossible to use in the operating room as sensors would have to be implanted into the patient. The data recorded from such sensors is a combination of both the left and right instruments which makes it more difficult to analyze.

In addition to the forces and torques between the tool tip and hand, the grasping force that is applied to the handle during the closing of the surgical tool has also been recorded [56, 9]. This force is captured by strain gauges on the handle of the instrument between the thumb position and the instrument shaft (Figure 2.6). The strain gauges do not add any burden to the surgeon, but the difficulty of installing and calibrating the strain gauge has prevented their widespread adoption.

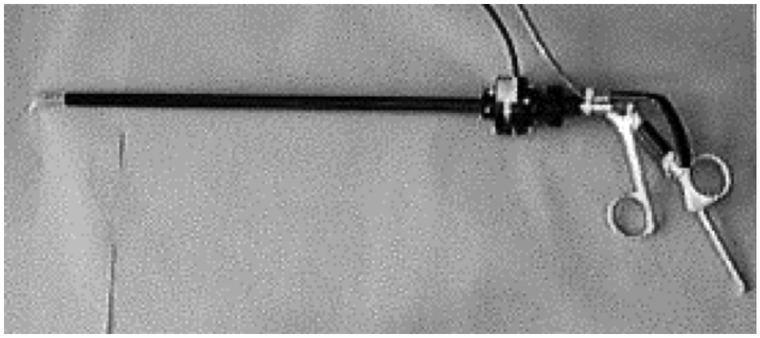

Figure 2.6: Strain gauge mounted on the handle of the surgical tool to capture grasping forces, from Brown et al. [9].

2.3 Measures of Skill

Raw data from the systems is complex and must be processed to provide a useful analysis of movements and forces. The most common analysis is the use of *global measures*, or descriptive statistics, which reduce an entire procedure into a single number. Some of these measures, such as total time and total path length, can be used to distinguish novices from experts but they cannot be used to describe qualitatively how the movements differ. A *local analysis* can provide a qualitative description by comparing motion paths, or other signatures, such as force.

2.3.1 Global Measures

To date, most research into objective surgical skill evaluation has focused on global measures. These measures are usually simple to compute and to compare between groups. Some measures can be used more reliably than others to discriminate between groups regardless of the task and the hand being analyzed. Chmarra et al. provide a brief overview of measures used in assessment, such as path length, motion smoothness, movement economy, deviation from ideal path and other measures from the 3D kinematics of the surgical tool [12].

Movement Quantity

The *total time* taken to complete a task is often the most reliable discriminator of surgical skill. This measurement requires no special recording equipment and can be applied to nearly any surgical task. Intuitively, the total time to completion is higher in novices, as they make more errors, perform more inefficient movements, and are generally more hesitant than experts. Total time has been shown to correlate with expertise in virtual reality, box trainers, and in the OR [17, 20].

The *path length*, L, of the instrument's trajectory, $\mathbf{p}(t) = \{x(t), y(t), z(t)\}$, is calculated as $L = \sum_t dist(\mathbf{p}(t), \mathbf{p}(t-1))$, and is widely used in the assessment of surgical skill. This measure is highly correlated with the total time, as a longer completion time tends to involve more movements of the instrument.

The ICSAD system introduced another measure, the *number of movements*, which was defined as a 'change in velocity' but the authors did not provide a definition of what constitutes a change [20]. Oostema et al. define "motion smoothness" in the same manner, but no additional details are given [44]. For example, one method may be to segment the movement based on some thresholds on the speed, e.g., a change in speed of 10% over the period of a few samples is considered to be a separate movement. Another method may be based on substantial changes in the direction of movement. Regardless of the method, the number of movements is likely to be correlated with the duration of the task. No attempts at normalizing this measure with respect to duration have been reported.

Another measure used by Chmarra et al. [16] is the movement of the instrument along the main axis of its shaft. This measure attempts to quantify the difficulty that novice surgeons have in determining depth information from the laparoscopic camera view, as they tend to misjudge depth and have to repeatedly reattempt grasping tasks. This measure increases as the duration of the operation increases, and no reports have been made with respect to normalizing this measure with respect to time. Cotin et al. [17] describe an equivalent measure for estimating a participant's ability to judge orientation by summing the angular rotations around the instrument's shaft. There was a visible difference in this measure when comparing novice and expert groups, but the difference was not confirmed statistically.

Movement Quality

In many tasks, experts tend to have smoother motions than novices [17]. This could be caused by novices making hesitant movements, having shaky hands, and a number of other factors. Several measures have been used to calculate smoothness. Chmarra et al. uses the third derivative of the position at time t, $\mathbf{p}(t) = \{x(t), y(t), z(t)\}$ to represent the changes in acceleration [16],

$$smooth_{Chmarra} = \sqrt{\frac{1}{2}\int_0^t \left(\frac{\partial^3 x}{\partial t^3}\right)^2 + \left(\frac{\partial^3 y}{\partial t^3}\right)^2 + \left(\frac{\partial^3 z}{\partial t^3}\right)^2 dt} \,. \tag{2.1}$$

Motion smoothness can also be calculated from the curvature of the signal, as in Judkins et al. [32]. The curvature of a motion path represents the tendency of the trajectory to maintain a straight line at every point in time and is calculated as

$$\kappa(t) = \left| \frac{\dot{\mathbf{p}(t)} \times \ddot{\mathbf{p}(t)}}{\dot{\mathbf{p}(t)}} \right| . \tag{2.2}$$

A point along a straight line has $\kappa = \infty$, and a point inside an abrupt change in direction would have a very small κ value. Significant differences were found between novices and experts, in a comparison of the median values and 95% confidence intervals of curvature in a robotic surgery environment. Pellen et al. [50] and Ritter et al. [57] found significant differences between novices and experts with the ProMIS measure of motion smoothness, defined as the 'cumulative number of instrument accelerations'. This measure may be more related to the ICSAD's number of movements measure, but it is difficult to tell in the absence of detailed descriptions.

Virtual Reality trainers offer additional evaluation measures, as they can precisely monitor and control the simulated virtual objects and tissues. Buzink et al. [10] describe experiments performed with the GI Mentor II training system, and they found differences between novices and experts in the number of collisions with tissue walls and the proportion of time a virtual patient was in pain. In experiments with the LapSim system, Kundhal and Grancharov [33] found significant correlations between the amount of tissue damage in the virtual trainer and the tissue damage during a live procedure on humans. They also found correlations between economy of motion scores such as angular path and path length in virtual environments and similar measures in live surgical procedures. These results show that these measures, while being artificial constructions and difficult to standardize, have the potential to be useful predictors of skills in the OR.

Force Based Measures

Attempts to discriminate skill levels using global measures of force have met little success. By placing a 6 DOF force/torque sensor underneath a synthetic artery, Dubrowski et al. [25] found that experts apply significantly higher average forces than novices, but this study lacked specific details on how the average force was calculated, whether it was the mean value or mean absolute value, and which axes were included. The higher average force may be explained by the fact that experts were likely in contact with the tissue and thus applying force for a greater proportion of the time, as it has been shown that novices spend more time in an idle state [62]. Another study also found that novices apply a higher average force, but this claim was substantiated only by a plot of a single stitch from an novice and an expert [69]. These findings are in contradiction to a study by Hwang et al. that found no significant difference between experts and novices when looking at the mean force recorded from a 3-axis sensor mounted inline with the surgical instrument [31].

Brown et al. [9] analyzed the grasping mechanics of novices and expert surgeons during operations on animal models, but were unable to find a clear distinction between the groups. The authors of the paper suggest that more complex modelling techniques, e.g., Hidden Markov Models, are needed to analyze grasping force data.

2.3.2 Local Analysis

Local analyses of surgical movements provide a more detailed comparison between operations as they consider the paths of the trajectories and the movement patterns. This level of analysis can be used to differentiate between skill levels and to provide more detailed feedback to trainees on their performance. Reiley et al. [55] provides an overview of these techniques in their review of surgical skill evaluation.

Movement Segmentation

Complete medical operations are often too complex to analyze as a whole and must be decomposed and segmented into smaller, more manageable units. Different approaches have been taken to segmentation depending on the complexity and type of the activity being analyzed. A single procedure can be segmented into a number of tasks, and each task further segmented into a number of movements, called *surgemes* [54]. It is possible to further reduce each surgeme into a combination of *dexemes*, which are individual motor movements, but a clear taxonomy is not available for the movements at this level. This structure closely mimics natural language, where paragraphs (operations) are composed of sentences (tasks), and sentences are composed of words (surgemes) that are in turn composed of phonemes (dexemes).

Automatic segmentation of a full operation into its constituent tasks allows the workflow of an operation to be monitored by a computer [8, 48]. The constituent tasks of each full operation vary depending on the type of operation. Bouarfa, Jonker and Dankelman [7] proposed a decomposition of the laparoscopic cholecystectomy (gall bladder removal) operation into 13 tasks: incision and hasson-trocars insertion, trocars insertion, laparoscopic instruments insertion, gallbladder preparation, neck release, clipping, cutting, gallbladdder removing, optics displacement, gallbladder packaging in endobag, instruments and trocars removing, endobag and hasson-trocars removing, and suturing. These steps are not standardized and vary between institutions, and a number of alternative models have been proposed [47, 8].

The segmentation of a task into surgemes is the most prevalent approach to modelling surgical skills. Typically, a few representative tasks such as suturing or positioning of the gallbladder are chosen to be further segmented into surgemes. Rosen et al. [59, 60] use a vocabulary of 15 surgemes to describe the movements in three separate tasks within a laparoscopic cholecystectomy: idle, closing, opening, pushing, rotating, closing - pulling, closing - pushing, closing - rotating, pushing - opening, pushing - rotating, rotating - opening, closing - pulling - rotating, closing - pushing - rotating, pushing - rotating - opening and closing - spinning. Some of these may be better classified as dexemes, but there is no formal taxonomy that provides a clear distinction between surgemes and dexemes. A detailed decomposition of the motions involved with a typical suturing operation can be found in a study by Cao and MacKenzie [11]. This study identified 13 surgemes that are involved in the suturing process, e.g., 'position needle', 'bite tissue', 'pull suture through', 'form loops'. This classification distinguishes between surgemes and dexemes more clearly, as each of the surgemes involves a number of smaller movements. The position needle surgeme, for instance, requires several movements to orient the needle in the grasper and align it with the tissue.

Only one study has explicitly examined the use of dexemes for modelling minimally invasive surgery [53]. This study compares the performance of a Hidden Markov Model (HMM) trained on labelled surgemes with a model trained on unlabelled dexemes during a robotic suturing task. The HMM trained on the labelled surgemes performed slightly better (100% compared to 95%), but required manual labelling of the input data.

Movement Features

The data used to model surgical operations has a tremendous impact on the effectiveness of the resulting model. Kinematic and dynamic data from the sensors is complex, and these high-dimensional data sets often contain redundant information. To make use of the data, it must be simplified into a more manageable form that represents the movements performed. This lower-dimensional form is referred to as a set of *features*.

At the coarsest level of analysis, e.g., full procedures, the input data is usually quite simple and the most common signals are the tools that are currently in use. These signals can be acquired either through offline video analysis or through sensors placed on the instruments. With this approach, the feature vector at every point in time consists of an N-dimensional binary vector, where N is the total number of instruments used in the operation and each value represents whether or not that tool is in use [5].

Analyzing movements at the surgeme and dexeme level requires more data than just the tools used, as numerous movements and tasks can be completed with the same instruments. The data used at this level comes from the motions of the tools and the forces applied to them [65, 36, 63]. Studies with the Blue DRAGON system use a 13-dimensional feature vector containing angular velocities, forces, torques and a binary value specifying whether the tool is in contact with the tissue [59]. Larger feature vectors are found in studies analyzing robotic surgeries, where velocities, angles, and positions are known for both the surgeon-robot and patient-robot interface, resulting in feature vectors that can exceed 70 values per sample [37].

Large feature vectors typically contain a substantial amount of redundant data that can negatively impact the modelling of the surgical process. A variety of data reduction techniques are used to project the high dimensional feature vectors into a lower dimensional space. Some data reduction processes are quite complex, involving a multi-stage operation that replace a number of dimensions with their combined magnitude, perform a vector quantization operation and then builds a codebook from the resulting vector [59]. Other approaches have applied a Short Time Fourier Transform to the kinematic data followed by vector quantization [65] or have used a Linear Discriminant Analysis [37]. Simpler techniques, such as using the centroid distance function (CDF) have been used to map 3D positional data to a 1D representation [36]. The CDF replaces each value with its distance from the centroid of the motion trajectory. No single technique has been shown to be generally applicable to all data sets.

Modelling

Building a model of the surgical process involves finding a pattern that relates the feature vector to each of the segments. The most successful modelling tool has been Hidden Markov models (HMMs) [59, 63, 36, 65]. HMMs are statistical models that have been very successful in modelling human speech and gestures, processes which are very similar in nature to the movements of a surgeon. An introduction to Hidden Markov models within the context of laparoscopic surgery modelling can be found in Rosen et al. [62].

An HMM is defined as $\lambda(\mathbf{A}, \mathbf{B}, \pi)$, with $\mathbf{A}$ being the transition probabilities to and from each of the N states, with B being the set of probability density functions for each observation from each state, and π is the probability of initializing the model in each state. HMMs are built on Markov chains, which are representations of a process by a set of N discrete states $S = \{s_1, s_2, ...s_N\}$, where the current state of the model is determined only by the previous states. In Markov chains, the state of the process is directly observable and the only parameter to define is the transition probabilities $\mathbf{A} = \{a_{11}, a_{12}, ..., a_{NN}\}$, where a_{ij} is the probability of transitioning from s_i to s_j. Within the context of surgical procedures, these states often represent surgemes and a Markov chain represents a full task.

With Hidden Markov models, the state of underlying Markov chain is not directly available and must be inferred from observations generated by each state. Each state, s_j, defines a probability density function, $b_j(k)$, for generating a given observation, k. In surgical procedures, these observations are the feature vectors at different points in time. This abstraction is needed, as the system is not directly aware of which surgeme is currently being executed by the surgeon, so it must use the data available from the sensors to try and estimate the most likely surgeme. A simple HMM with three states is depicted in Figure 2.7.

Rosen et al. [62] describe the three 'problems of interest' with respect to HMMs in surgical evaluation. The first problem is optimizing the parameters ($\mathbf{A}$, $\mathbf{B}$, π) to best model a set of observations. This is the process of building a model of a surgical task from recorded data. Another problem of interest is computing the probability of a set of observations given a model, $P(O = o_1, o_2, ..., o_T|\lambda)$. This is equivalent to finding the probability that the data from the recorded surgery came from the same data that built the model. The last problem of interest is computing the hidden sequence of states given an observation sequence and a model, $\mathbf{P}(S = s_1, s_2...s_T|\lambda, O)$. This is equivalent to determining what the sequence of surgemes are from recorded data.

Skill Classification

The simplest measure of skill classification from local analysis is to calculate the order of execution and time spent performing the various stages. This can potentially be used at the operation level as well as lower segmentation levels [61]. This anal-

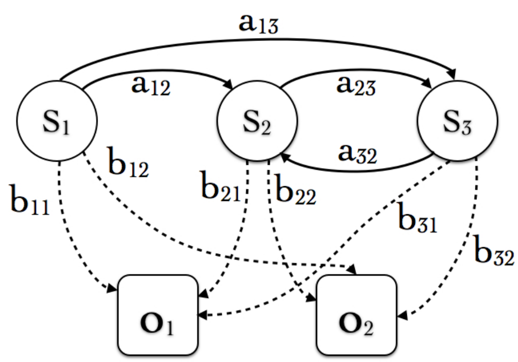

Figure 2.7: Sample Hidden Markov model with three states and two observation vectors.

ysis is similar to the global measures of movement quantity as novices spend more time in each state. Local analysis can also provide a more qualitative assessment of skill. For example, Rosen et al. [61] found that novices spent much more time in the *idle* state than experts, indicating that they may take more time to transition between movements and plan out their actions.

Another method of quantifying the surgical skill based on a local analysis is the comparison of models built from novice training data with models built from expert training data [59]. The model of each novice is compared against the model of each expert using a statistical distance function. This distance function sums the probability that the expert's movement came from a model trained on novice movements, and the probability that the novice's movements came from a model trained on expert movements. The distance between each novice and expert was then compared against the average inter-expert distance. A strong correlation ($r = 0.86$) was found between the statistical distance and a subjective evaluation by an expert. This result suggests that there is some similarity between experts not only in the time taken to perform tasks but also in the movements used to complete the tasks, as the inter-expert distance was lower than the average novice-expert distance.

Chapter 3

Data Capture System

3.1 System Design

A data capture system was developed to record all of the data from the motion tracking system, the force and torque sensors, the video streams, and the microphone. The central component of the system consisted of the PC with four gigabytes of RAM and a quad-core CPU to process the large quantity of data. The PC ran Windows XP which was required for compatibility with the motion tracker and force and torque sensor. A schematic diagram of the system is depicted in Figure 3.1. A multi-threaded C++ program interfaced with all of the devices.

Synchronization of the data was achieved through the use of the Windows system time as a global clock. This clock has a resolution of 15ms, which is not sufficient for directly time-stamping all of the force measurements, but it does allow for interpolation of the values for intermediate samples. The position measurements and video were recorded at 20 Hz and 30 Hz respectively, and the physical movements that were recorded are relatively slow (a few centimetres per second), so this synchronization method did not pose a problem.

Participants performed the required surgical tasks in an Endo-trainer from 3D-Med [1] (Figure 3.2). This trainer simulates a laparoscopic surgery environment with a small movable camera to simulate a laparoscope, and rubber holes that simulate the trocars used in real laparoscopy. Synthetic tissue or other items are placed inside the Endo-trainer to be manipulated by the participants using laparoscopic instruments. The only modification to the Endo-trainer was the placement of a video

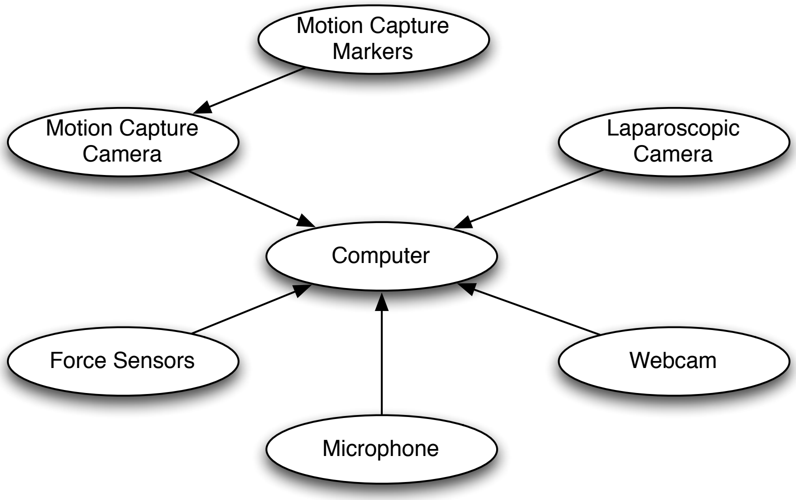

Figure 3.1: Schematic overview of system components.

splitter on the camera output to allow the video to be recorded.

3.2 Motion Tracking

The Visualeyez II VZ3000 optical motion tracker from PTI Phoenix [51] was used to capture the participants' movements. Three cameras placed linearly on a tripod were used to triangulate the position of each of the infrared markers. The VZ3000 is able to uniquely identify up to 64 points by sequentially flashing each marker so the cameras only capture a single marker in each frame. While using fewer markers can achieve higher frame rates, the effective capture rate was 20 Hz with the required 64 markers.

The markers were tracked with 0.7 mm root mean square error [51]. The tracking volume was defined by a horizontal and vertical angle of 45°, extending out approximately 7 m. Though the tracking volume can be increased through the use of multiple camera units, the experiments were conducted with a single camera unit.

Each of the markers was connected to the wireless transponder module (Figure 3.3) of the VZ3000 system. This module synchronized the activation of the infrared markers with the camera unit using an RF signal, and provided the participant more comfort and freedom than the wired version. Each participant wore the transponder

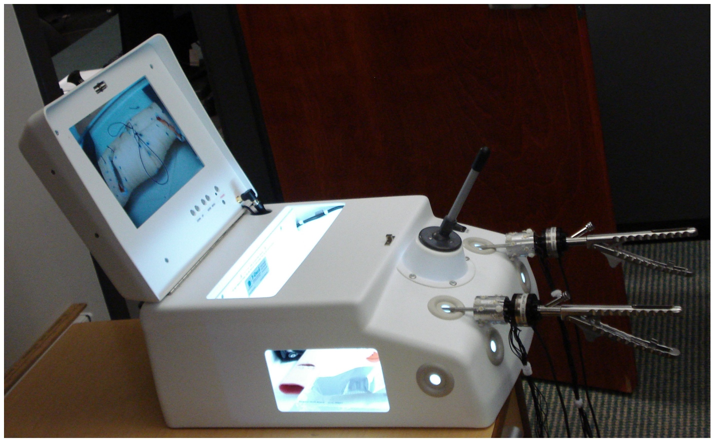

Figure 3.2: Endo-trainer from 3D-Med used in the studies.

on a belt, so the markers were tethered to the participant rather than the computer.

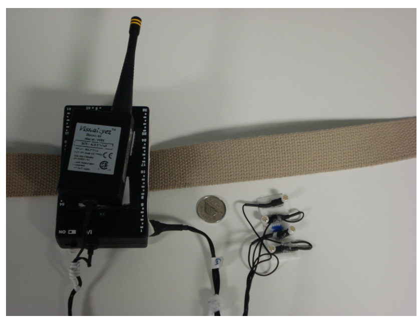

Figure 3.3: Infrared markers with wireless transponder unit.

The VZ3000 software provided access to the motion data through the C++ API provided by Phoenix PTI. This API connected to the VZ3000 recording software and retrieved the data from the currently running capture session. The API only supported a polling method for retrieving data, not an event-based method. This required the tracker to be persistently checked for updated locations. Since the effective capture rate was 20 Hz, a single loop in C++ polled the tracker for new values at the Nyquist rate of 40 Hz, which is the minimum sampling frequency required in order to ensure there is no aliasing of the signal. After each data frame is retrieved through the API, the marker positions were written to a flat text file along with the system timestamp.

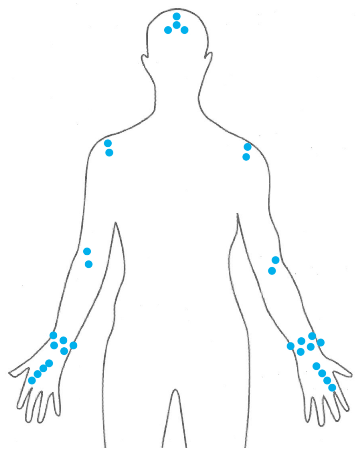

Figure 3.4: Diagram of marker placements.

3.2.1 Marker Placement

In total, 64 markers were fixed to the equipment and the participant for each trial. This configuration was chosen so the position and orientation of the needle drivers, which are the laparoscopic instruments used in the trials, as well as the participants' hands, wrists, elbows, shoulders, and the Endo-trainer could be tracked. A diagram of the marker placements on the participants is shown in Figure 3.4.

The position and orientation of the needle drivers was computed from the locations of the markers that were fixed to each tool. Twelve markers were attached to an aluminum collar (32 mm diameter, 48 mm height) (Figure 3.5) in two equally spaced rings. Each of the two rings contained six markers, spaced 11 mm apart; the rings were 16 mm apart. The collar was attached to the shaft of the needle driver using plastic screws. The marker configuration allowed the instrument to be tracked as it was moved through the tracking volume, as the tracking unit needs to only see three of the markers to accurately determine the tool tip location using the templating process described in Section 3.2.2.

Four markers were secured to the dorsum of each of the participants' hands on the skin above the second metacarpal using a double-sided carbon fiber adhesive tape. The position of these markers allowed the system to resolve the two degrees of freedom of the hand (radial/ulnar deviation, and elevation/depression). While only two markers were necessary to capture this motion, additional markers provided

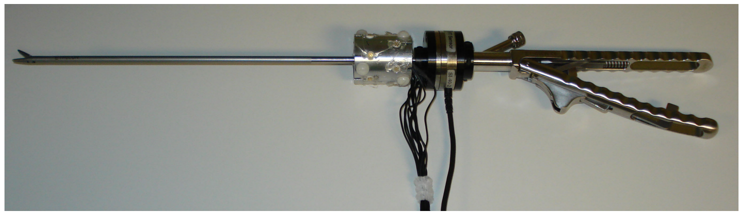

Figure 3.5: Collar with infrared markers and force sensor mounted on laparoscopic needle driver.

redundancy in cases of occlusion or tracker malfunction. The markers also come bundled in groups of four, making it inconvenient and cumbersome to place the additional markers elsewhere.

The position and orientation of each forearm was tracked using eight markers fixed to an elastic strap worn over the wrist. The markers were arranged uniformly in a similar fashion to the collar used for the needle drivers, and a templating process similar to the one described in Section 3.2.2 was applied to determine the position and orientation of the forearm.

Each elbow and shoulder joint was tracked using two markers. The elbow markers were secured to the medial side of the elbow using double-sided carbon fibre adhesive tape. The markers on the shoulders were secured using a velcro strap in conjunction with a harness to prevent the markers from slipping. While only one marker is needed to track the position of each joint, a second marker provides redundancy. Most of the movement of the upper body, including shoulder abduction/adduction, elevation/depression, protraction/retraction, elbow flexion/extension, and pronation/supination can be captured from the shoulder, elbow, and wrist markers.

The position and orientation of the head was tracked using four markers attached to the participants' head using a velcro strap. Three of the markers were arranged in an equilateral triangle, with the fourth marker placed in the centre. The normal to the plane intersecting the three markers in the triangle can be used to represent the orientation of the head. The location of the fourth marker in the centre of the triangle can be used as the position of the head. The distance between this marker and the centroid of the triangle can be used to estimate tracking error.

Four markers were fixed to the Endo-trainer in an identical arrangement to those used to track the head. These markers allowed the surgical field to be located within the tracking system's reference frame.

3.2.2 Instrument Tracking Using Templates

The Endo-trainer occludes the surgical field from the viewpoint of the tracking unit making the tool tip impossible to track directly, so the position of the tool tip was extrapolated from the positions of the markers on the collar around the tool. Prior to the trials, a template was created that relates the positions of the markers on the collar to the position of the tool tip. The resulting template had a total of 13 positions, 12 for the collar, and 1 for the tool tip.

In order to track the tool tip relative to the collar when building the template, an additional marker was required on the tip. The instrument was then moved around the tracking volume and rotated to ensure that all markers were made visible to the camera tracking unit. During this process, all position data was recorded to disk for offline processing.

The templates were initialized by finding the frame that has the largest number of markers visible and storing this as the reference frame for the instrument's coordinate system. Subsequent markers were added to the template by finding additional frames that included 'unseen' markers, as well as at least three markers that were included in the reference frame. The markers that are visible in both frames were used to find a rigid-body transformation, which is a rotation and translation, $T_{trk \to ins} = R_{trk \to ins} \cdot \mathbf{p} + \mathbf{t_{trk \to ins}}$ by finding a least-squares solution to minimize the Euclidean distance between corresponding points. The resulting transformation was then applied to the unseen point to transform it from the tracker coordinate system to the instrument coordinate system. This process was repeated until all thirteen markers had been moved into the instrument coordinate system.

Pseudo-code for templating process is given in Algorithm 1. The algorithm is run on a recording of N samples of each of the 13 marker positions in tracker space, Trk. The algorithm produces an array of 13 marker positions in template space, Tpl. The variable $unseen$ stores boolean values to track which markers have

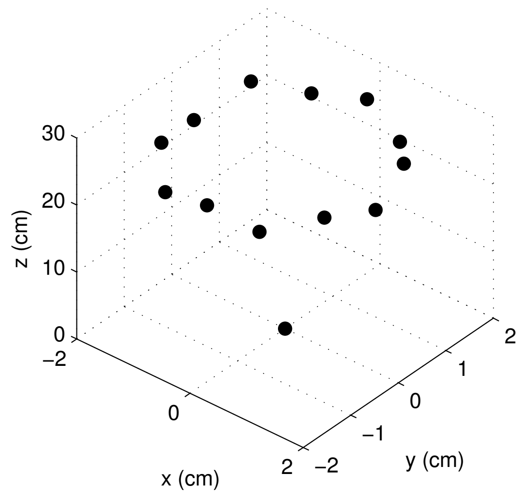

Figure 3.6: Example of an instrument template constructed from the measured data.

been added to the template. The $isVisible(i, n)$ function returns true if marker i is visible in frame n of the recording, the $findAlignment(A, B)$ function returns a rotation and translation $[R, \mathbf{t}]$, that aligns the corresponding points in A and B. An example of a resulting instrument template is depicted in Figure 3.6. The ring of the twelve markers on the collar is visible at the top of the image, and the tool tip position is visible at the bottom, at (0,0,0).

3.2.3 Filtering

The raw data retrieved from the VZ3000 system contained a substantial amount of erroneous data due to the physical connections on the wired markers becoming loose. A sample of these errors is shown in Figure 3.7. In addition, there are frames with insufficient data, e.g., when only two markers on an instrument are visible. To mitigate the impact of the erroneous and missing data, a number of filtering operations were performed. The filtering operations are shown in Figure 3.8 and described below.

The process for constructing the templates was quite sensitive to errors, so a strict approach to filtering this data was taken. This filter was very similar to a median filter in that it first sorts the data within a window of $ws = 19$ around each data point. Then, if all three axes of each of the N data points, $\mathbf{p}(t)[1:3] =$

Algorithm 1 Instrument templating algorithm

```
maxIndex ← n that maximizes Σ_i isVisible(i, n))

% Use the found frame to initialize the template.
for i = 1 to 13 do
   if isVisible(i, maxIndex) then
      Tpl[i] ← Trk[i]
      unseen[i] ← 0
   end if
end for

% Add all of the unseen markers to the template.
for x = 1 to 13 do
   if unseen[x] = 1 then
      maxVisibleWith, maxVisibleIndex ← −1

      % Find the frame with the most markers visible and already in the template.
      for n = 1 to N do
         visibleWith ← 0
         for y = 1 to 13 do
            if unseen[y] = 0 and isVisible(y, n) then
               visibleWith ← visibleWith + 1
            end if
         end for
         if visibleWith > maxVisibleWith then
            maxVisibleWith ← visibleWith
            maxVisibleIndex ← n
         end if
      end for

      % Find alignment between the frame and the template.
      templatePos, trackerPos ← {}
      for i = 1 to 13 do
         if unseen(y) = 0 and isVisible(i, maxVisibleIndex) then
            templatePos ← templatePos ∪ Tpl[i]
            trackerPos ← trackerPos ∪ Trk[i]
         end if
      end for

      % Apply alignment to the marker to move it into template space.
      [R, t] ← findAlignment(templatePositions, trackerPositions)
      Tpl(x) ← R · Trk[x] + t
      unseen[x] ← 0
   end if
end for
```

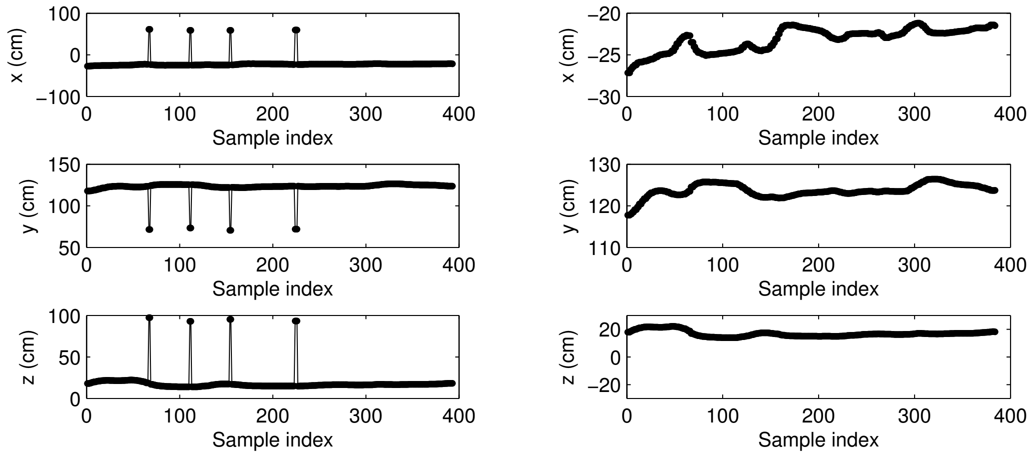

(a) Raw position data, with outliers visible.

(b) Position data with outliers removed.

Figure 3.7: Filtering outliers.

$[x(t), y(t), z(t)]$ were not sorted into one of the three centermost positions, the point was considered an outlier and thus discarded. This approach resulted in many data points being discarded, but few data points were actually needed and it was essential that all data be accurate. The pseudo-code for this algorithm is given in Algorithm 2.

Algorithm 2 Median discard filter

for $i = ws/2$ to $N - ws/2$ **do**
  $window = p(i - ws/2 : i + ws/2)[1:3]$
  $error \leftarrow 0$
  for $k = 1$ to 3 **do**
    $s \leftarrow sort(p[i - ws/2 : i + ws/2][k])$
    if $(p(i)[k] < s[\lfloor ws/2 \rfloor - 1])$ or $(p(i)[k] > s[\lceil ws/2 \rceil] + 1)$ **then**
      $error \leftarrow error + 1$
    end if
  end for
  if $error == 2$ **then**
    $p(i)[1:3] \leftarrow NULL$
  end if
end for

When filtering the data from the participant's movements, the system was less sensitive to noise and data was filtered using an ad-hoc filtering method. This filter iterates over each sample point, and discards the point if it is more than half the

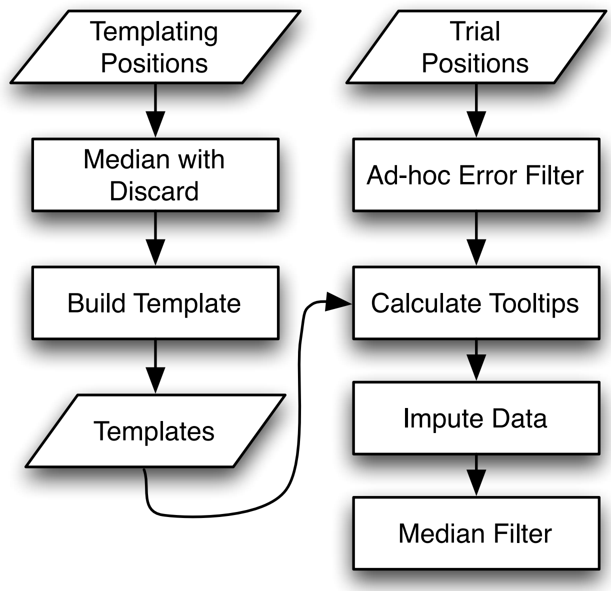

Figure 3.8: Filtering operations used to compute the final position of each tooltip.

variance from the mean of the signal. Following this, a standard median filter with a window size of $ws = 15$ filters the resulting signals for each marker. This approach removed most, but not all of the noise from the signal, and preserved the majority of the signal.

In order to obtain a relatively smooth and continuos signal, data was imputed at locations where data was unavailable due to occlusion, or had been discarded by the filtering process. This data was imputed using a simple linear interpolation operation, generating samples in a straight line between the two neighbouring positions where data was available. This imputed data is over-simplistic and not representative of the true movements, but it makes up a very small portion of the final data and has little effect on the outcome.

3.3 Force and Torque Data

Each needle driver was instrumented with a force and torque sensor (Figure 3.5) positioned between the tool tip and the handle of the tool to capture the interaction between participant and tissue. The force detected by the sensor was the sum of the tool tip-tissue forces, the force generated by the friction on the rubber trocar, and the weight of the shaft of the needle driver and motion capture markers.

3.3.1 Force and Torque Transducer

The Mini40 force and torque sensor from ATI Industrial [3] contains six strain gauges that respond to the load that is applied to the instrument. The voltages from the strain gauges are recorded by the computer, and later processed into calibrated force and torque readings. This sensor was calibrated to provide accurate force sensing in the range of -35 N to 35 N in the x and y axes, and -106 N to 106 N in the z axis, with less than 0.3 N error in all axes. The torque was calibrated to a range of -1.5 Nm to 1.5 Nm in all axes with less than 0.008Nm error. The z axis is aligned with the instrument shaft, the x and y axes are perpendicular to this axis and each other.

The sensor was sampled using the NI-PCI 6224 data acquisition card from National Instruments [43], with a sampling rate of 1000 HZ and 16 bits of resolution using the NI-DAQmx C interface provided by the manufacturer. Data was stored in a buffer on the card, and read into the CPU 100 samples at a time. To accurately timestamp each of the 100 recordings, linear interpolation operation detailed in Algorithm 3 was used. This timestamping allows for the synchronization of force data with the video and position data.

Algorithm 3 Force timestamp interpolation

$curTime \leftarrow globalClock()$
$readSamples()$
for $i = 1$ to 100 **do**
  $timestamp(i) \leftarrow prevTime + i * (curTime - prevTime)/100$
end for
$prevTime \leftarrow curTime$

The voltages from the strain gauges in each of the force transducers were transformed into force and torque measurements at the tip of the instrument using a 6x6 matrix provided by the manufacturer. This matrix converts the raw voltages to calibrated force measurements, and transforms the location of the force and torque measurements from the centre of the force sensor to the tool tip. This matrix was applied to the voltages during the post-processing of the data, so the system was not additionally taxed during the data acquisition. The resulting values are the force and torque recordings in the force coordinate system, $\mathbf{F_f}$.

Due to the mechanics of the sensor and its position on the needle driver, the force generated by closing the handle on the instrument saturates the recordings along the length of the shaft. This makes it impossible to measure the true force applied by the participant in the z axis, but there is likely very little information in this data for the particular tasks that were analyzed. The z component of the force was thus eliminated before analyzing the applied forces. The benefit of this configuration is that the large spikes in the force can be used to detect when the participant opens and closes the handle.

3.4 Coordinate Systems

There are three separate coordinate systems that needed to be unified in order to provide a meaningful analysis of the data: tracking system, template, and force sensor. The tracking coordinate system was the native reference frame of the motion capture system and had its origin about the centre of the camera unit and measured x, y, and z in cm. The template coordinate system was similar to the tracking coordinate system, but the location of the origin varied with the data used to construct the template. In that coordinate system, only the relative positions between the markers were important. The force sensor reference frame was centred around the tool tip with forces in x, y, and z measured in N, torques around those axes measured in Nm.

The common coordinate system was chosen to be the tracking coordinate system. In order to unify all coordinate systems, the template of the instrument was first aligned with the force and torque coordinate system following the template construction. Then, a rigid body transform was computed to align transform measurements from that coordinate system into the tracking coordinate system.

3.4.1 Alignment of Template with Force and Torque

To be able to transform the force and torque measurements from their local coordinate system into the tracker coordinate system, the instrument coordinate system was aligned with the force and torque coordinate system. Since the measurements use different units, only the orientation of the axes were considered. Since the force reported in the z axis was already calibrated to respond to force along the instrument's shaft, only the x and y axes were aligned.

Aligning the two coordinate systems involved translating the tool tip position to the origin (0,0,0) and aligning the z axis with the shaft of the instrument. Alignment of the z axis was achieved by rotating the instrument about the origin such that the centroid of all of the markers on the collar was in line with the positive z axis, i.e., the x and y components of the centroid were 0.

To complete the alignment, the instrument template needed to be rotated around the z-axis. The angle of rotation was found by securing the instrument parallel to the ground, recording the force measurements in this position and then hanging a weight on the tool tip as depicted in Figure 3.9. Subtracting the initial measurement from the measurements when the force was applied gives the direction of the force in the force reference frame. Since only the x and y axes needed to be aligned, placing the instrument parallel to the ground ensures that the z axis component of the force applied by gravity is zero. The instrument, as well as the position of the weight, was motion-captured and forces were recorded during this procedure, providing the direction of the force applied in tracker space, $\mathbf{F_{trk}}$, and the direction of the force in force space $\mathbf{F_{frc}}$. The dot product of $\mathbf{F_{trk}}$ and $\mathbf{F_{frc}}$ represents the angular offset between the force sensor and instrument template. By rotating the template by the resulting angle, the axes of the instrument coordinate system become aligned with those of the force coordinate system.

3.4.2 Alignment of Template with Tracker

The application of the template to compute the tool tip position used a process similar to the template construction. On every frame, correspondences between

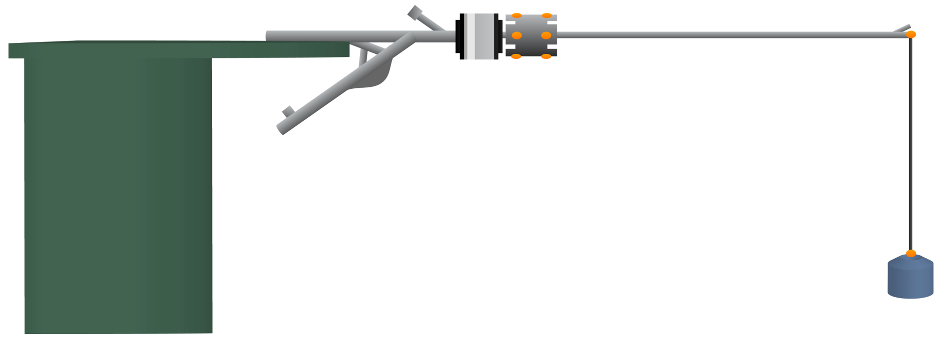

Figure 3.9: Configuration used to calculate the rotation needed to align the template and force coordinate systems.

the visible instrument markers and the markers in the force-aligned template were found. A rigid body transform $T_{ins \to trk} = R_{ins \to trk} \cdot \mathbf{p} + \mathbf{t_{ins \to trk}}]$ that minimized the distance between these correspondences was computed using a least-squares method. If less than three markers were visible in the given frame, it was marked as having no data and filtering operations were used to impute data for it.

To compute the tool tip position in tracker coordinate system, the transform $T_{ins \to trk}$ was applied to the tool tip position in the force-aligned template. To compute the force in the tracker coordinate system only $R_{ins \to trk}$ was applied to the force and torque recordings. The translation was omitted, as the force and position are aligned only in the orientation of their reference axes, not in the scale and units of the axes.

3.5 Video and Audio

3.5.1 Video

Two separate video streams were captured to provide a reference for later analysis. Videos were captured using the OpenCV library [45], encoded using the DivX encoder [22], and written directly onto the disk. In addition, a flat text file was created that stored the timestamp for each frame to provide a means to synchronize the video with the motion and force data. Both video streams were recorded and processed on the same thread in the CPU.

One video stream was recorded using a standard web camera, the Logitech

QuickCam Orbit MP [39]. This camera recorded video at 30 frames per second with a resolution of 320x240 pixels. The camera was focussed on the participant's upper body and hands. This information was useful for the expert surgeon evaluating the performance of the participant and as reference when comparing the movements to the recorded trajectories.

The second video stream recorded the view from the laparoscopic camera located in the Endo-trainer. This was accomplished by splitting the signal from the laparoscopic camera and routing it to a Syntek STK 1135 USB video capture card. The use of the splitter allowed the video to be captured by the PC while still displaying on the screen of the Endo-trainer. The USB capture card generated video at a resolution of 640x480 pixels, at 30 frames per second.

3.5.2 Audio

Audio of the recording events was captured using a standard desktop microphone and the LiveInCode [38] program. The audio was not significant for the analysis of the participant, but was captured to ensure that the entire process was recorded as completely as possible.

3.6 Data Processing

Several of the measures used in the analysis require further processing of the data. All data processing was performed offline using MATLAB 2009b [41].

3.6.1 Curvature

The curvature of a 3D trajectory is a 1D signal that describes how the trajectory changes direction in space. This is a useful representation of the data, as it is of lower dimension than the original signal and is invariant to rotation and translation. The curvature is used to estimate motion smoothness, as well as perform a local analysis on the movements.

Curvature Background

Let $\mathbf{f}(t) = \{x(t), y(t), z(t)\}$ be a function that defines a trajectory in 3D space with respect to time, t. The parametrization of the path by time means that motion paths are not time invariant, and paths that follow identical trajectories at different speeds are substantially different. To avoid this problem the path can be reparameterized by arc length, s, allowing trajectories of identical paths to be represented identically, even if executed at different speeds. This new representation of the trajectory, $\mathbf{p}(s)$ can be calculated with the following mapping from time to arc length,

$$s = \int_0^t \sqrt{\left(\frac{\partial x}{\partial t}\right)^2 + \left(\frac{\partial y}{\partial t}\right)^2 + \left(\frac{\partial z}{\partial t}\right)^2}\, dt\,. \tag{3.1}$$

This conversion to arc length also prevents large spikes in the curvature calculation when the instruments are relatively still. These spikes introduce large variation into the resulting signal, and make analysis and signal comparison very difficult. The conversion to arc length should not remove information that is contained in the time-domain representation of the signal, as this conversion is similar to a time-normalization operation. Because of this, computations of motion smoothness, and gesture comparison using the curvature signals should not be affected.

The derivative of the trajectory, $\mathbf{T} = \frac{\partial \mathbf{p}}{\partial s}$, is the tangent vector and represents the direction of the trajectory. The second derivative of this function is the normal vector, $\mathbf{N} = \frac{\partial^2 \mathbf{p}}{\partial s^2}$, and is perpendicular to the tangent vector. The cross product of these two vectors, $\mathbf{B} = \mathbf{T} \times \mathbf{N}$ is the binormal vector, and is perpendicular to both. These three vectors (Figure 3.10) form the Frenet-Serret frame, which is a mathematical construct that describes a trajectory in 3D space. Within this frame, one can define the intrinsic parameters of curvature and torsion.

The curvature, κ, of a trajectory in space is a one dimensional signal that describes how the tangent vector changes direction within the spanning plane of $\mathbf{T}$ and $\mathbf{N}$. The magnitude of the curvature is

$$\kappa = \frac{||\frac{\partial \mathbf{p}}{\partial s} \times \frac{\partial^2 \mathbf{p}}{\partial s^2}||}{||\frac{\partial \mathbf{p}}{\partial s}||^3}\,. \tag{3.2}$$

In the simplest case of a 2D trajectory with the curvature constant and equal to zero, the path is a straight line. When the curvature of a path is constant and non-

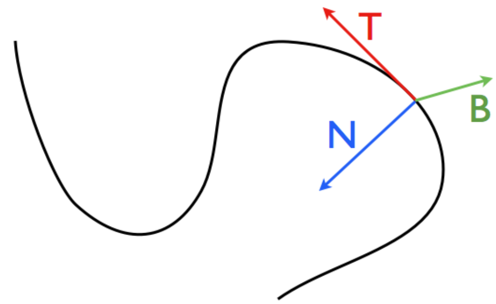

Figure 3.10: The vectors $\mathbf{T}$, $\mathbf{N}$ and $\mathbf{B}$ of the Frenet-Serret frame.

zero, then the path is a circle with a radius of κ^{-1}. Complex curves have κ values varying between $-\infty$ and ∞. Extending this concept of 2D curvature into 3D space requires *torsion*, denoted τ. The torsion of a trajectory represents the tendency of the curve to leave the plane spanned by $\mathbf{T}$ and $\mathbf{N}$. The magnitude of the torsion is

$$\tau = \frac{||\left(\frac{\partial \mathbf{p}}{\partial s} \times \frac{\partial^2 \mathbf{p}}{\partial s^2}\right) \cdot \frac{\partial^3 \mathbf{p}}{\partial s^3}||}{||\frac{\partial \mathbf{p}}{\partial s} \times \frac{\partial^2 \mathbf{p}}{\partial s^2}||^2}. \tag{3.3}$$

A path with constant curvature and constant torsion is a helix, an arbitrary path in 3D space has $-\infty \leq \kappa, \tau \leq \infty$.

Curvature and torsion are intrinsic properties of the trajectory, and as such are invariant to rotation and translation. These factors as well as the time invariance from the arc length parameterization make curvature and torsion robust descriptors of the curve geometry. Curvature has been proven useful in analyzing real-world gestures from sensors [42]. Torsion is less useful, however, as each derivative from sensed data increases the noise in the signal, and the torsion calculation requires a third derivative. Most trajectories are relatively co-planar as well, so torsion was not used in the analysis of the recorded data.

Calculation of Curvature from Recorded Signal

Calculation of the curvature from the filtered data positions involves a multi-stage process. The first stage is the conversion from the time-domain to the arc length domain. Next, the positions are uniformly resampled within the arc length domain. The positions are further filtered with derivatives of a Gaussian low-pass filter which serve to smooth the data and compute the derivative in a single step. The resulting smoothed positions are then used to calculate the curvature signal. This process is executed four times with different window sizes for the Gaussian low-pass filter so the trajectories can be analyzed at a number of scales.

Each of the recorded positions was assigned an arc length index using a discretized version of Equation 3.1. This parameterization produced a non-uniform sampling in the arc length domain, as fast movements produce much greater changes in arc length than slow movements when sampled at constant time. A uniform sampling was required for the derivative calculations, so the resulting arc length domain signals were then resampled at a uniform interval of 5 mm, using linear interpolation where required. This resampling interval preserved the majority of the signal. Resampling was performed by applying Algorithm 4 to each of the instrument tip positions, with $\mathbf{p_{arc}}$ being the Winsorizing domain trajectory with N samples and Winsorizing indices $\mathbf{s_{arc}}$, $\mathbf{p_{uni}}$ the trajectory with uniform Winsorizing with M samples and Winsorizing indices $\mathbf{s_{uni}}$:

Algorithm 4 Uniform resampling of trajectory in arc length

$M \leftarrow totalPathLength/5mm$
for $i = 1$ to M **do**
  $s_{uni}(i) \leftarrow (i-1) \cdot 5mm$
  $below \leftarrow max(\mathbf{s_{arc}} < \mathbf{s_{uni}}(i))$
  $above \leftarrow min(\mathbf{s_{arc}} > \mathbf{s_{uni}}(i))$
  $ratio \leftarrow (\mathbf{s_{uni}}(i) - \mathbf{s_{arc}}(below))/(\mathbf{s_{arc}}(above) - \mathbf{s_{arc}}(below))$
  $p_{uni}(i) \leftarrow \mathbf{p_{arc}}(below) + ratio \cdot (\mathbf{p_{arc}}(above) - \mathbf{p_{arc}}(below))$
end for

The derivatives of the instrument trajectory were calculated and low-pass filtered in a single, efficient operation. The filtered first derivative of the trajectories, $\frac{\partial \mathbf{p}}{\partial s}$ was calculated by convolving each of the dimensions (x, y and z) with the first derivative of a Gaussian kernel with a window size of ws and standard deviation of σ. The filtered second derivative of the trajectories, $\frac{\partial^2 \mathbf{p}}{\partial s^2}$ was calculated by convolving each of the dimensions with the second derivative of a Gaussian kernel with a window size of ws and a standard deviation of σ.

$$\frac{\partial \mathbf{p}}{\partial s} = \mathbf{p_{uni}} * s \cdot e^{\frac{-s^2}{2 \cdot \sigma^2}} , \tag{3.4}$$

$$\frac{\partial^2 \mathbf{p}}{\partial s^2} = \mathbf{p_{uni}} * \frac{s^2 - \sigma^2}{\sigma^4} \cdot e^{\frac{-s^2}{2 \cdot \sigma^2}} . \tag{3.5}$$

The parameters ws and σ were left as free parameters so the trajectories could be analyzed at different scales. Four scales were used in the analysis: Scale 1 with $ws = 31, \sigma = 3$, Scale 2 with $ws = 31, \sigma = 9$, Scale 3 with $ws = 51, \sigma = 19$, Scale 4 with $ws = 99, \sigma = 35$. The finest scale, $\sigma = 3$, was chosen as it smoothed out most of the noise in the signal while preserving the majority of the movements. With smaller values of σ, the noise overwhelmed the signal. The largest scale, $\sigma = 35$, filtered out the smaller movements, leaving only the larger, more deliberate motions. Any larger values of σ resulted in over-smoothing and loss of important data. These values were chosen using an ad-hoc visual inspection of their effects on a sample of recorded data.

The curvature value used in the analysis was calculated as

$$\kappa_p = \ln \left(\frac{|| \frac{\partial \mathbf{p}}{\partial s} \times \frac{\partial^2 \mathbf{p}}{\partial s^2} ||}{|| \frac{\partial \mathbf{p}}{\partial s} ||^3} \right) . \tag{3.6}$$

Each scale was calculated using the same equation, resulting in four curvature signals for each of the instrument trajectories. The logarithm function was used to compress the range of the curvature values, as it is unbounded. Without it, very small changes in the velocity ($\frac{\partial \mathbf{p}}{\partial s}$) result in extremely large curvature values that prohibit a meaningful analysis. Examples of the calculated curvature values are shown in Figure 3.11, and are overlaid on the 3D trajectories in Figure 3.12.

3.6.2 Mechanical Energy

The measure of mechanical energy combines the force and position information to estimate the energy applied by the surgeon during the tasks. This measure is referred to as work within the context of physics, but can be thought of as the energy used in the manipulation of the tissue. This does not represent all energy expended by the surgeon, as only the energy measured at the instrument is considered, not the kinetic energy of movement through free-space, or any other energy exerted by the

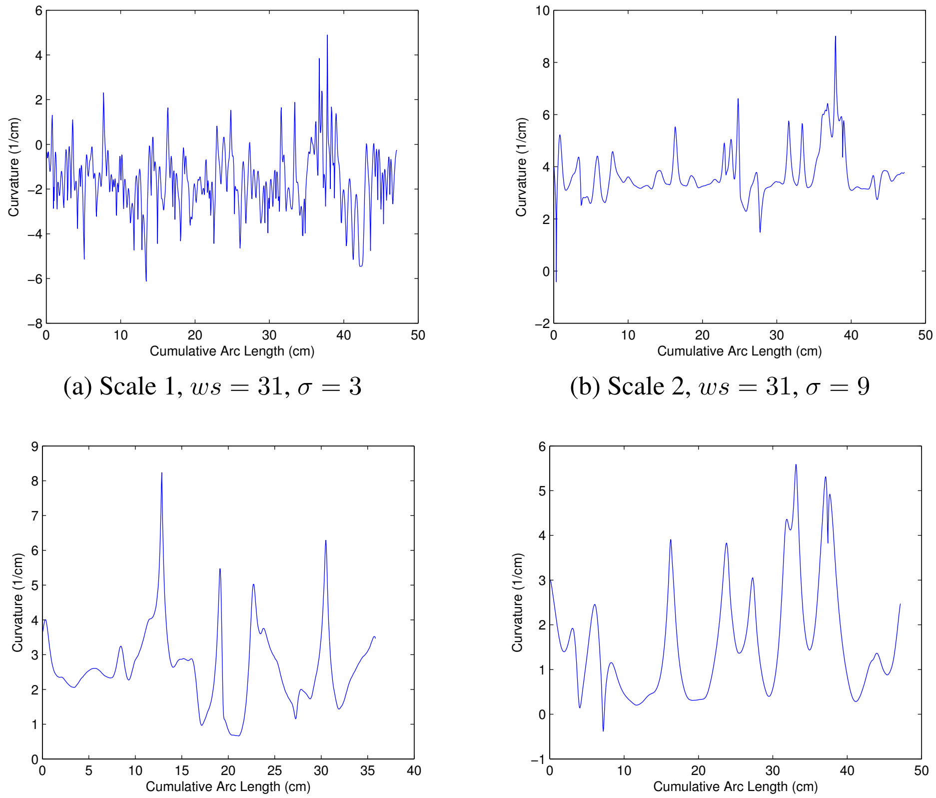

(a) Scale 1, $ws = 31$, $\sigma = 3$

(b) Scale 2, $ws = 31$, $\sigma = 9$

(c) Scale 3, $ws = 51$, $\sigma = 19$

(d) Scale 4, $ws = 99$, $\sigma = 35$

Figure 3.11: Plots of the curvature calculated from the insertion segment.

surgeon. This measure was meant to capture the movement economy of a surgeon, as expert surgeons should execute more efficient maneuvers as they develop their skill. It should also capture the care in which the tissue is handled, as peaks in the energy used may damage delicate tissue.

Energy was computed from the force and tool tip position value in the tracker coordinate system. Before computation, the position data was smoothed with a Gaussian filter with a window size of $ws = 31$ and a standard deviation of $\sigma = 4$ to remove measurement noise. The change in energy between sample points was computed as

$$E_t = (F_t - F_{t-1}) \cdot (p_t - p_{t-1}) \,. \tag{3.7}$$

Examples of the signals used to compute the energy, and the resulting energy signals are shown in Figure 3.13.

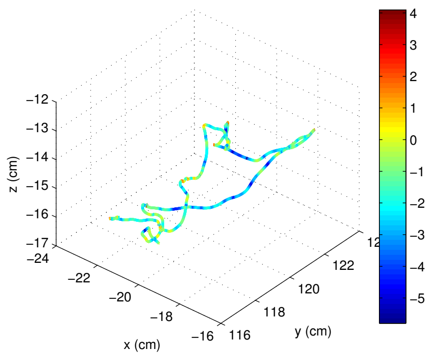

(a) Scale 1, $ws = 31$, $\sigma = 3$

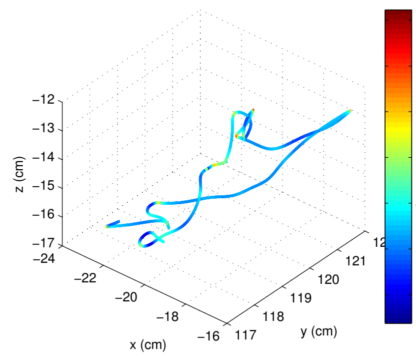

(b) Scale 2, $ws = 31$, $\sigma = 9$

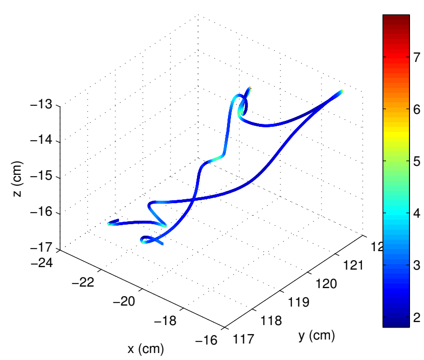

(c) Scale 3, $ws = 51$, $\sigma = 19$

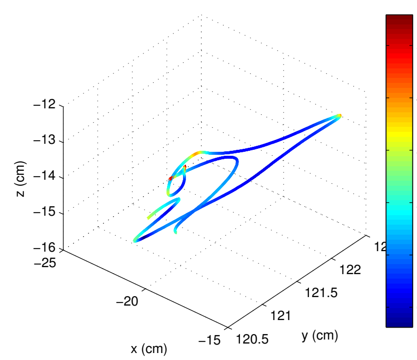

(d) Scale 4, $ws = 99$, $\sigma = 35$

Figure 3.12: 3D plots of the insertion segment, with curvature shown as colour. Trajectories have been smoothed with Gaussian filters with the ws and σ values of the corresponding scale.

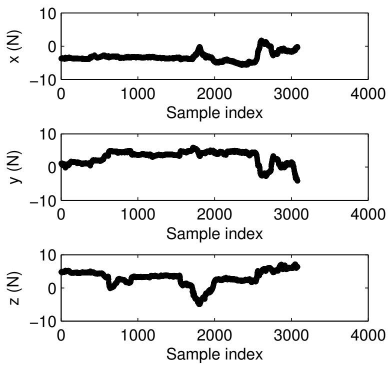

(a) Force signal from a simple interrupted suture.

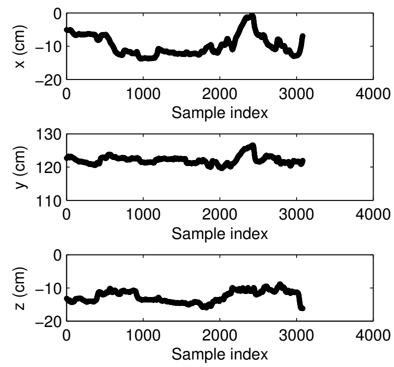

(b) Position signals from a simple interrupted suture.

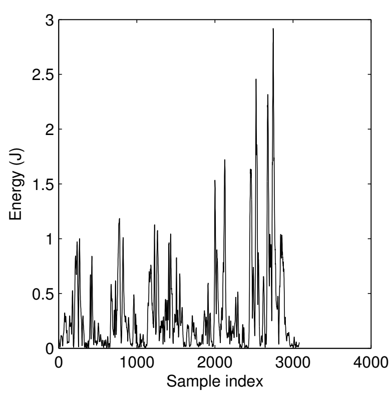

(c) Energy signal from a simple interrupted suture.

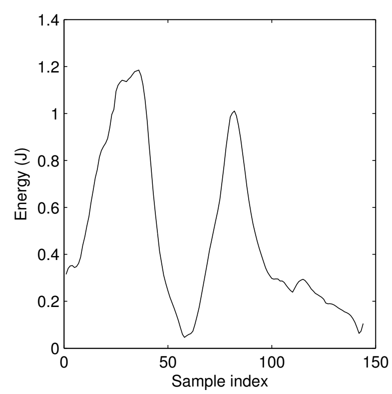

(d) Energy signal from the 'pull through' segment of a simple interrupted suture.

Figure 3.13: Example energy signal, and the force and position signals used in its computation.

Chapter 4

Experimental Methodology

4.1 Procedure

An empirical study using the system was conducted at the Center for the Advancement of Minimally Invasive Surgery in Edmonton, Alberta. Ethics approval for the study was obtained from the University of Alberta and Alberta Health Services. Thirteen participants were involved in the study, each receiving $50 for their participation. Participants were recruited through an email sent to all general surgery and urology residents, as well as in person during their regular surgical training sessions.

The data from three participants was removed due to technical problems (excess sunlight on the infrared markers and a miscalibrated tool template), leaving complete datasets from ten participants. The participants represented a broad range of skill levels (residents from all five years of residency, surgical fellows, and staff surgeons). All participants were male.

After signing a written consent form, participants were asked to complete a questionnaire, a stereo vision test, and a manual dexterity pegboard task. Then participants were fitted with the motion capture equipment and asked to complete the Fundamental Laparoscopic Skills pegboard task, a series of simple interrupted sutures, and a continuous running suture. Finally, participants were asked to fill out a second questionnaire requesting a self-evaluation of their performance.

4.1.1 Questionnaire

Participants completed a two page questionnaire that included questions relating to demographics, training level, and other factors that may affect performance. Questions relating to demographics and training included age, gender, dominant hand, vision, and current training status (year of residency, fellowship, staff surgeon).

Self-assessments of their own skills in open surgical procedures and in laparoscopic surgical procedures was recorded on a five point Likert scale with relevant 'anchors' for each of the five points. For example, in self-assessing their skills in open surgery, participants could select 1 - No experience, 2 - I have practiced on synthetic tissue; I have learned the basic skills, 3 - I am confident with my skills; ready to suture in the OR on patients, 4 - Experience performing full operations, or 5 - Expert surgeon. These anchors were developed in conjunction with an expert surgeon to ensure they reflected a reasonable set of responses.

Participants were also asked about surgical training their and recent events which may have impacted their surgical dexterity. Regarding their training, they were asked to estimate the number of times they had performed a laparoscopic cholecystectomy or a laparoscopic fundoplication (common laparoscopic operations), and the number of days since they had practiced laparoscopic surgery. They were also asked if they play video games or regularly perform other tasks requiring fine motor skills, the number of hours of sleep they had missed in the last week, and the number of caffeinated drinks they had consumed in the last 24 hours.

4.1.2 Stereo Vision Test

The stereoacuity of each participant was assessed using the RanDOT stereo vision test [52]. For this test, participants were asked to wear polarized glasses and view a series of ten images (Figure 4.1). In each of the images, there were three circles, one of which is comprised of two separate circles separated by a small (varying) distance. Through the polarizing glasses, these two circles appeared as a single circle that stood out from the other two. Participants were asked to identify which of the three circles appeared to stand out from the others. The images are presented with decreasing disparity, making it more difficult to perceive which circle stood out. The first incorrect response was taken to be the participant's stereoacuity limit.

Figure 4.1: RanDOT stereo vision test, used to measure stereoacuity.

4.1.3 Manual Dexterity Pegboard

Manual dexterity was assessed using the Purdue Pegboard [49]. This is a standardized test that is used to assess fine motor skill in a variety of domains including industrial work and rehabilitation. Participants complete the task by placing as many pins as possible into the holes on the pegboard (Figure 4.2) within 30 seconds. The test was administered according to the instructions provided for the 'left', 'right' and 'simultaneous' conditions, as described below.

For the first subtask, the 'right' condition, participants were instructed to pick up a single pin from the small bowl at the top of the board with their right hand, and place it into the first hole on the right hand column of the board, and repeat the process as quickly as possible. They then placed 3-5 pins for practice before the experimental trial was performed. The 'left' condition was administered similarly, but with the left hand and left column on the board. For the 'simultaneous' condition, participants used both hands in tandem, picking a pin from both the left and right bowl at the same time, and placing them into both columns on the board. The conditions were executed in the same order (left, right, simultaneous) for all participants.

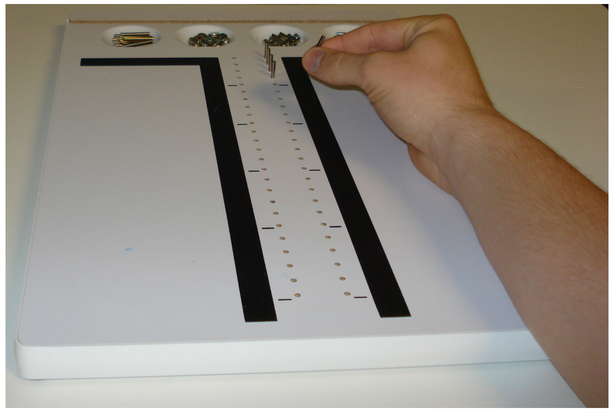

Figure 4.2: Purdue Pegboard, used to measure manual dexterity.

4.1.4 Fundamental Laparoscopic Skills Pegboard

The Fundamental Laparoscopic Skills pegboard is a standardized task that is currently used to assess the laparoscopic dexterity of surgeons. The FLS pegboard task consists of moving a number of coloured, rubber collars from one side of the board (Figure 4.3) to the other using laparoscopic instruments. Evaluation is completed by an observer who records the event duration and the number of pegs that are irretrievably dropped. These two measures can be used to calculate a very coarse measure of laparoscopic skill.

The FLS pegboard task was used as it is a very simple task that participants of all skill levels can understand and complete. Participants were instructed to complete the task as it is normally administered, i.e., lifting a collar off a peg with the left instrument, transferring to the right instrument, and placing the collar on a peg on the right hand side of the board. Participants used the instrumented needle drivers described in Section 3.3 instead of the curved laparoscopic graspers that are typically used for the task. This made the task slightly more difficult, but allowed the force and torque to be recorded while the task was completed.

Participants were given the opportunity to practice by transferring a few pegs from left to right and back again before completing the trial. They were given no specific instructions e.g., to focus on speed or accuracy, and no time limit was imposed.

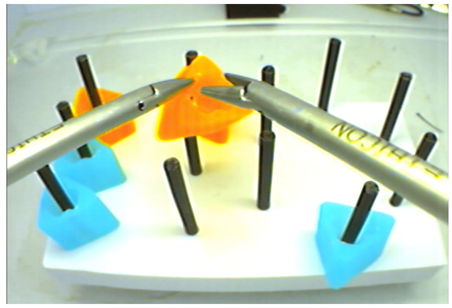

Figure 4.3: Pegboard task from the FLS program.

4.1.5 Simple Interrupted Sutures

A simple interrupted suture is a type of knot used in surgical procedures to connect tissue. It is composed of two bites (when a needle enters the tissue) and a number of throws (the individual 'knots' used to secure the suture). It is a relatively common operation used for training laparoscopic skills, and all participants were familiar with this type of suture. This task requires a fair bit of coordination to place and secure the suture properly. It is substantially more difficult than the pegboard task but easier than the continuous running suture.

The sutures were placed in a piece of synthetic bowel tissue. Participants were asked to close a small hole that had been cut in the bowel by inserting five simple interrupted sutures at marked points around the hole. The marked points were 5 mm from the edge of the hole, and 1cm away from the neighbouring holes. A template was used to mark the points and the hole. All participants performed one warmup suture before completing the five trial sutures. Figure 4.4 shows the synthetic tissue with the markings before and after the simple interrupted sutures were inserted.

Participants were provided with 15 cm of 5-0 braided silk thread for each of the five sutures. This type of thread does not have 'memory' like the synthetic monofilament suture that is also used for laparoscopic procedures, so it is easier to work with.

Participants were instructed to insert the needle into the tissue with their dominant hand. They were also asked to complete the knot using three throws. The first throw was a double throw (two loops of thread around the instrument), the second and third throws were single throws (one loop of thread around the instrument). This is a standard method of the simple interrupted suture. After each suture, participants removed the needle and excess thread using laparoscopic scissors before beginning the next suture.

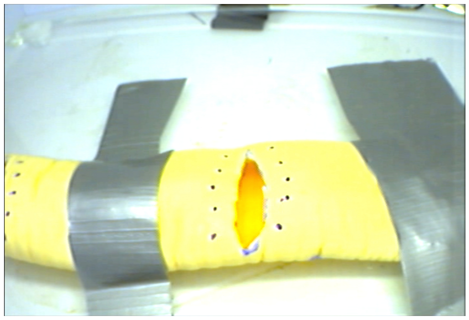

(a) Synthetic tissue prior to the task.

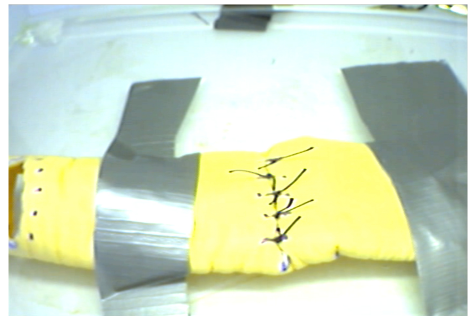

(b) Stitches placed in the synthetic tissue.

Figure 4.4: View from laparoscopic camera during simple interrupted suture task.

4.1.6 Continuous Running Suture

In the final task, the participants were asked to perform a continuous running suture. The continuous running suture is used to close a hole using a single thread. In the first step, the thread is secured with a knot at one end of the hole. After the thread is secured at the top, it is repeatedly inserted into the tissue along the hole to join the two edges, as depicted in Figure 4.5. At the end of the hole, the thread is tied back on itself to secure the entire suture in place.

This type of suture is quite difficult for a number of reasons. The longer thread (30 cm instead of 15 cm) is more difficult to manipulate laparoscopically. Participants must also plan their stitch more carefully, ensuring that there is enough thread left at the end to complete the final knot. Further, the final knot is tied to thread that is already inserted into the tissue, and it is thus more difficult to perform. Most participants were also less familiar with this type of suture, as it is not as commonly used as the simple interrupted suture.

Before beginning the task, participants were given the opportunity to view a video of an expert surgeon performing a continuous running suture. This was done to ensure that participants knew how to complete the task, as some had forgotten the required steps. Participants were not given the opportunity to practice this type of stitch, as it was performed after the simple interrupted sutures and participants had already had a chance to perform laparoscopic sutures.

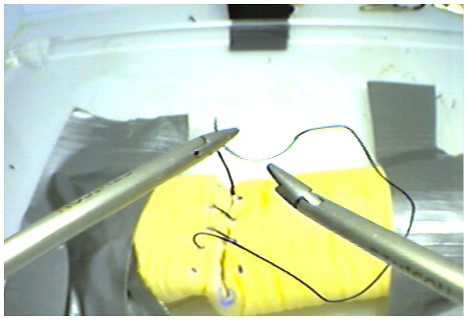

(a) Participant is midway through the task.

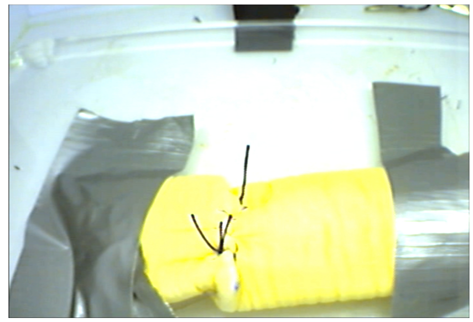

(b) Participant has completed the task.

Figure 4.5: View from laparoscopic camera during continuous running suture task.

4.1.7 Second Questionnaire

Following the continuous running suture, participants were asked to self-evaluate their performance on all of the tasks they had just performed using a five point Likert scale.

4.2 Subjective Data Analysis

4.2.1 Segmentation

Suturing is a complex procedure and is difficult to analyze without decomposing it into smaller movements. This decomposition was done by analyzing the time-stamped videos from the laparoscopic camera view. First, the videos of the simple interrupted suturing from all participants were analyzed in order to determine what movements are involved in laparoscopic suturing. The following movements were identified for simple interrupted sutures:

1. *Insertion* - This is the process of inserting the needle through the tissue. This movement involves penetrating one side of the hole that is being closed, pulling the thread through, and penetrating the other side of the hole. Depending on the surgeon and the location of the suture, the process of pulling

the thread through after the first penetration is sometimes omitted, and both penetrations were done with a single movement. The start of the segment is when the needle first makes contact with the tissue. The segment ends when the non-dominant hand grasps the needle after penetrating both sides of the tissue.

2. *Pull through* - This movement is defined as pulling the thread through the synthetic tissue. The segment starts when the non-dominant hand grasps the needle after penetration, i.e., the end of the insertion segment. The segment ends when the thread is completely pulled through the tissue and there is noticeable slack.

3. *Double throw* - In this movement, one instrument grasps the needle and uses it to loop the thread around the other instrument twice. The instrument without the needle then grasps the tail of the thread to prepare the throw to be locked in place. The segment starts at the end of the pull through segment. The segment ends when the instrument with the thread looped around it grasps the tail of the thread.

4. *Tighten suture* - This movement involves pulling the tail through the loops on the instrument and moving both ends of the thread away from each other to tighten the throw and lock it in place. The start of the segment is the end of a throw (either single or double). The segment ends when one end of the thread is released from the instrument.

5. *Single throw* - This is similar to the double throw, except that it only involves a single loop of thread around the instrument and occurs after a tighten suture movement.

6. *Collect tails* - This movement is used by the participant to arrange the ends of the thread and hold them upright so they can be cut. Sometimes a single instrument is used to grasp each of the tails sequentially, and sometimes both instruments are used. The segment begins following the last tighten suture movement and ends when the tails of the thread are held taut ready to be cut.

This taxonomy was applied to the videos using the defined criteria with a frame-by-frame analysis. An ideal suture would require each of the 6 sub-movements to be executed in the following order: Insertion, Pull through, Double throw, Tighten suture, Single throw, Tighten suture, Single throw, Tighten suture, Collect tails. Some of the non-experts were not able to properly complete all stages of the suture on the first attempt, and so some movements (e.g., Double throw and Tighten suture) were thus repeated several times in a single suture.

4.2.2 Expert Evaluation

After all participants had been recorded, the videos from the view of laparoscopic camera were provided to Dr. Daniel Birch, an expert surgeon, for evaluation. He viewed all of the videos and ranked them in order of perceived skill. No instructions were given, so the resulting evaluation was based solely on the expert's judgment. While only the instruments and tissue were visible in the video to provide anonymity, the expert was able to identify his own performance.

Chapter 5

Analysis and Results

Results from the questionnaire were analyzed, global measures were computed, and a local analysis was performed on the data recorded from the experimental trials. Previously established global measures, such as path length, total time, motion smoothness, and force features were compared to the newly defined energy-based measures. Local analyses of the curvature of the trajectory in space, and the energy signal were also performed.

5.1 Questionnaire and Non-surgical Tasks

Responses from the questionnaire were analyzed to check for any relation to expert-assessed surgical skill on the simple interrupted suturing task. All questions having numeric or Likert scale responses were considered. Data from all thirteen participants were included in this analysis, which was performed using Spearman's rank correlation coefficient. No significant correlations were found between expert assessed skill and any of the questionnaire responses.

The relationship between performance on non-surgical tasks and expert assessed surgical skill was analyzed using the Spearman's rank correlation coefficient as well. There was no relationship between performance on the stereoacuity test and surgical skill. There was also no relationship between surgical skill the number of pegs placed in the Purdue Pegboard under the 'right' and 'simultaneous' conditions. The number of pegs placed during the 'left' condition did show a positive correlation with surgical skill, but this was not significant ($\rho = 0.59$, $p = 0.08$)

5.2 Global Measures

Several global measures were computed from the three laparoscopic tasks, and their relation to surgical skill analyzed. Correlations were calculated between the measures and the expert-assessed ranking on the simple interrupted suture task. Expert assessments were not made for the FLS task or the continuous running suture task, but it was assumed that skill on the simple interrupted suture task would be indicative of skill on the other tasks. Correlations were computed using Spearman's rank correlation coefficient for non-parametric data.

5.2.1 Movement Quantity

Several measures of movement quantity were analyzed including total time, total path length, and total energy. The total time and path length are measures that have been previously shown to correlate with skill, and were used as a baseline to compare the new measure, total energy.

Total Time

The time required to complete a task has been shown to be a reliable measure of skill. Novices take more time than experts as they are more hesitant, less efficient, and are forced to repeat more movements due to errors. This metric is applicable to nearly all surgical tasks and can be computed without sophisticated measuring equipment. A drawback of this measure is that it is a very general assessment of skill, giving no feedback on how a surgeon can improve other than to 'go faster'.

Total completion time for each task was determined from a manual analysis of the captured video. For the FLS task, the start time was considered to be when the instrument touched the first collar, the end time was considered to be when the instrument released the last collar. For each of the simple interrupted sutures, as well as the continuous running suture, the start time was the beginning of the needle insertion, the end time was the end of the clip tails segment.

Completion time significantly correlated with expert-assessed skill ($p < 0.05$) on all three tasks. The strongest correlation was with the simple interrupted sutures,

($\rho = -0.84$, $p = 0.01$), the weakest with the FLS tasks ($\rho = -0.74$, $p = 0.02$). Figures 5.1a-c depict the total time for each task plotted against expert-assessed skill. These results are consistent with other studies in surgical skill evaluation. The strong correlation suggests that the expert evaluations of the participants are accurate, and that skill on the simple interrupted suture task is indicative of skill on the other tasks.

Path Length

The path length represents the distance that each tool tip travels through space as the task is performed. This measure can reflect the movement efficiency of the surgeon, as shorter paths indicate more economical movements. It can also reflect mistakes that are made, as repeating a number of movements will substantially increase the path length.

The path length for each task is independently computed from the positions of each tool tip using the data resulting from the filtering process described in Section 3.2.3. The length is computed as the cumulative sum of the Euclidean distances between sample points:

$$l = \sum_t \sqrt{(x(t) - x(t-1))^2 + (y(t) - y(t-1))^2 + (z(t) - z(t-1))^2}. \qquad (5.1)$$

The start and end time points were the same as were used when calculating total time.

A significant correlation was found between cumulative path length of the instrument in the dominant hand and expert-assessed skill for all tasks ($p < 0.05$). The path length of the instrument in the non-dominant hand was found to be significant for only the simple interrupted suturing task, not the FLS pegboard or the continuous running suture. This is consistent with other studies that have shown that measures of skill computed from the dominant hand are generally more discriminatory. The strongest correlation was found in the path length of the instrument in the dominant hand during the simple interrupted sutures ($\rho = -0.84, p < 0.01$). Computed path lengths for both instruments of all tasks are shown in Figures 5.2a-f.

Total Energy

The total energy measured should reflect the efficiency of the surgeon's movements, not only with respect to minimizing the path length, but the application of force as well. As with the other quantitative measures, total energy tends to increase as task duration increases. The calculation used for this measure is simply $E = \sum_t E_t$.

Contrary to most other measures in the literature and the ones analyzed in this study, total energy had a greater correlation with skill when analyzing the non-dominant hand, rather than the dominant hand. Both the FLS task and the simple interrupted sutures showed a significant negative correlation ($\rho = -0.79, -0.68$, $p < 0.05$) between expert-assessed skill and total energy for the non-dominant hand (Figures 5.3 b, d). A negative correlation was also found when analyzing the continuous running suture (Figures 5.3 e, f), as well as the dominant hand on all tasks (Figures 5.3 a, c, e), but these correlations were not significant. Total energy may not have the same discriminatory power as the other quantitative measures, but it appears to have some unique information not captured by the path length measure. Further tests with a larger sample size may reveal a stronger effect.

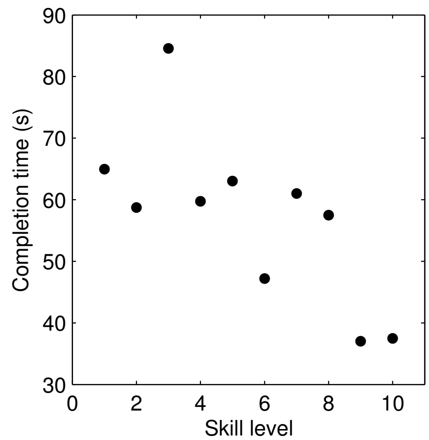

(a) Total time to complete FLS pegboard task.

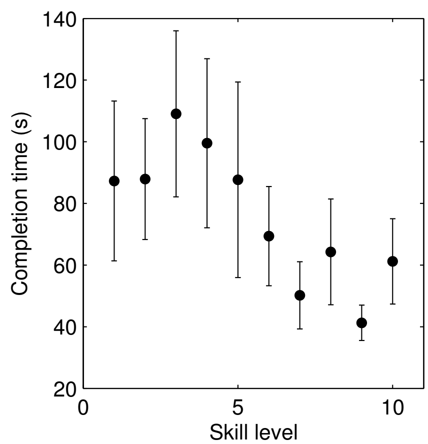

(b) Mean time to complete one simple interrupted suture, error bars indicate standard deviation.

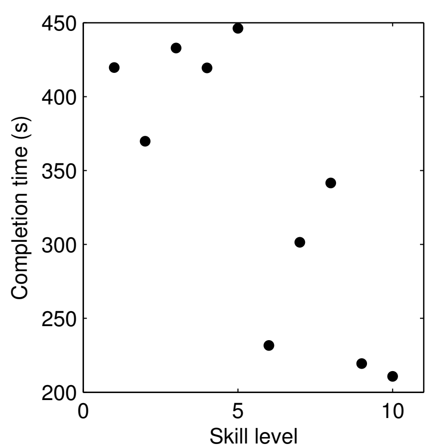

(c) Total time to complete continuous running suture.

Figure 5.1: Completion time for the performed tasks.

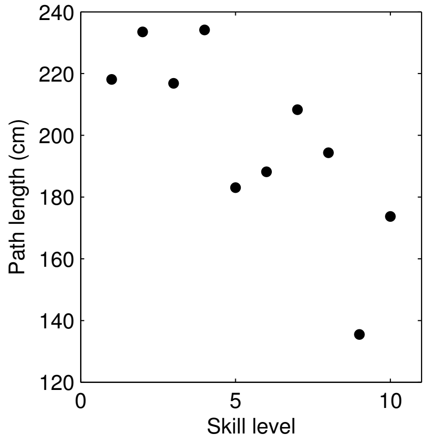

(a) Path length of instrument in dominant hand for FLS task.

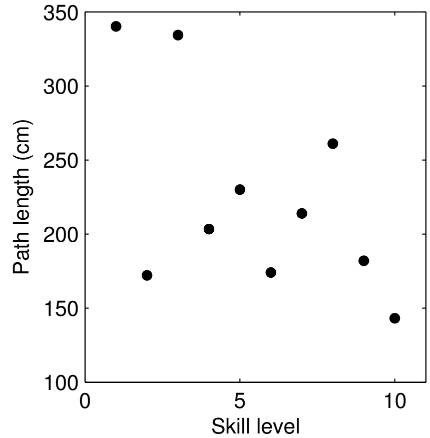

(b) Path length of instrument in non-dominant hand for FLS task.

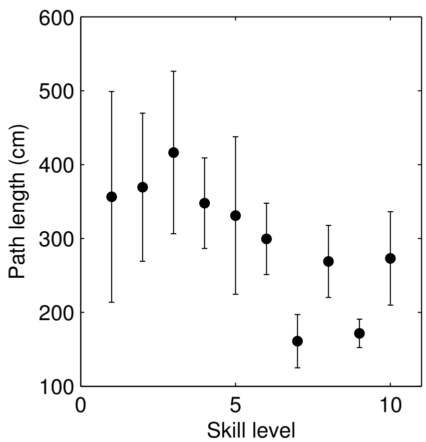

(c) Mean path length of instrument in dominant hand for simple interrupted suture task.

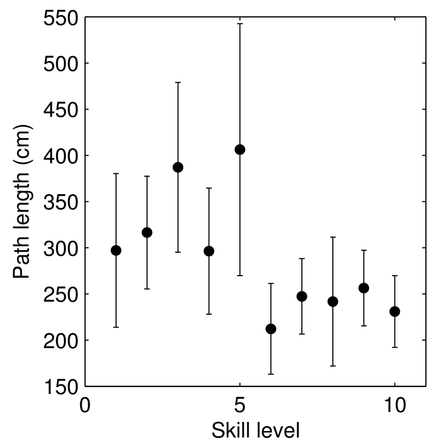

(d) Mean path length of instrument in non-dominant hand for simple interrupted suture task.

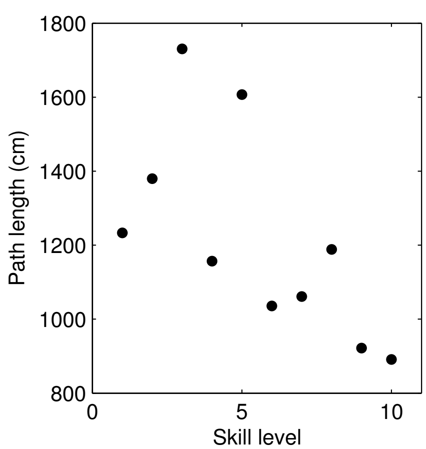

(e) Path length of instrument in dominant hand for continuous running suture task.

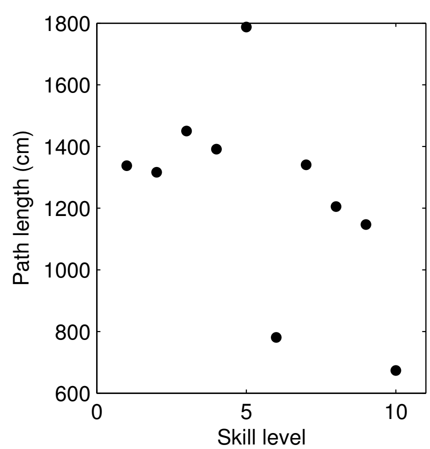

(f) Path length of instrument in non-dominant hand for continuous running suture task.

Figure 5.2: Path length for the performed tasks.

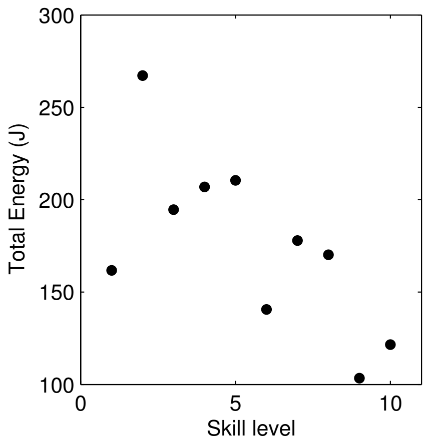

(a) Total energy from the dominant hand for FLS task.

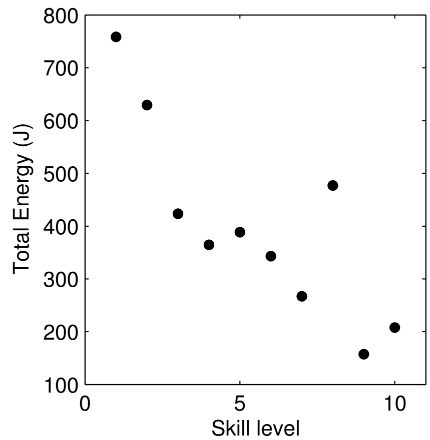

(b) Total energy from the non-dominant hand for FLS task.

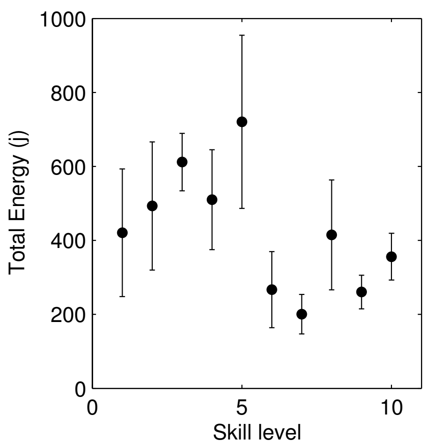

(c) Mean total energy from the dominant hand for simple interrupted suturing.

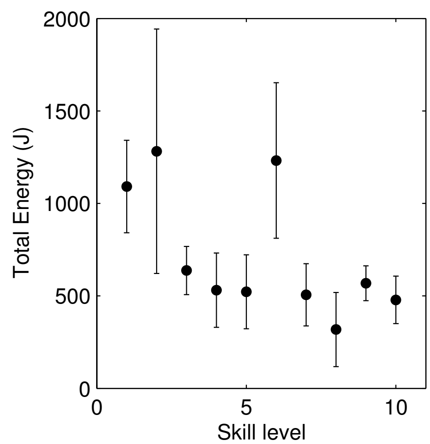

(d) Mean total energy from the non-dominant hand for simple interrupted suture.

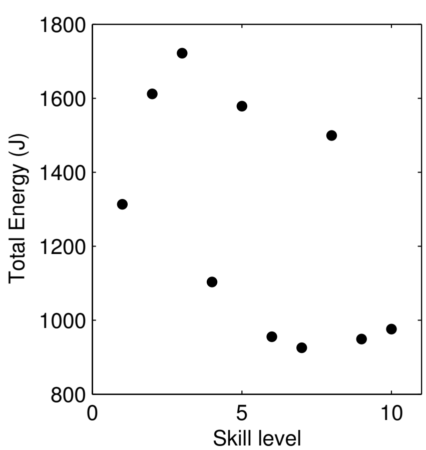

(e) Total energy from the dominant hand for continuous running suture task.

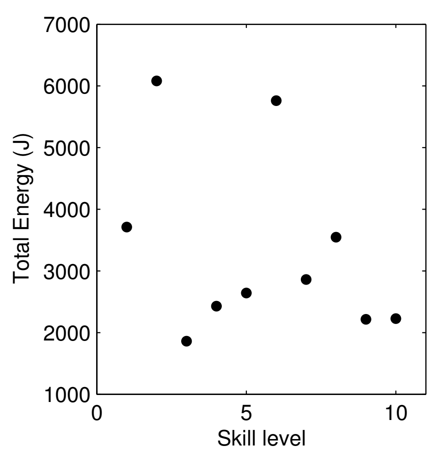

(f) Total energy from the non-dominant hand for continuous running suture task.

Figure 5.3: Total energy for the performed tasks.

5.2.2 Movement Quality

Motion Smoothness

Motion smoothness should reflect tremors in the hand and abrupt changes in the instrument's trajectory. It has been shown in prior studies that expert surgeons tend to have smoother motion paths. The motion smoothness was computed from the curvature signatures described in Section 3.6.1. From each curvature signature, the mean and median values are computed for each task.

No correlation was found between expert-assessed skill and the calculated motion smoothness for either hand. Both the mean and median and values were analyzed (Figures 5.4a-f and 5.5a-f), at all four scales of curvature. These findings are contrary to prior studies that did find a relation between motion smoothness from curvature in the dominant hand of some tasks [32].

Force and Torque

The forces applied by the participant can vary widely depending on the particular movements being executed. Low forces may be applied when manipulating tissue and high forces when tightening a suture. The variation makes it difficult to extract a reliable global measure that accurately reflects surgical skill. Both the mean and maximum of the magnitude of the force and torque values were computed.

No correlation was found between expert-assessed skill and the mean and peak force for each hand (Figure 5.6a-f and 5.7a-f). Similar results were found in the torque values. The results demonstrate the difficulty in extracting global measures from the complex force data.

Energy

To analyze the applied energy as a global measure of skill quality, the mean and peak of the energy signal were computed. Similar to the force measurement, no correlation was found between expert-assessed skill and the mean (Figures 5.8a-f) and peak of the energy signals. Given that the force and energy measures are quite similar, this is not surprising.

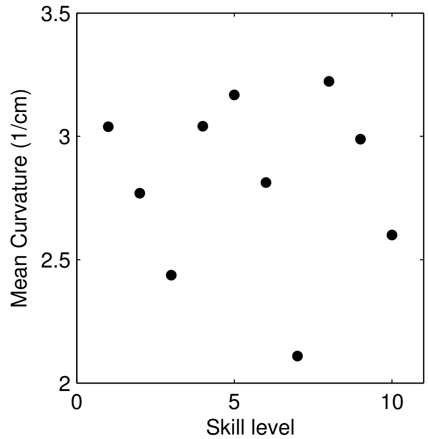

(a) Mean curvature of dominant hand for FLS task.

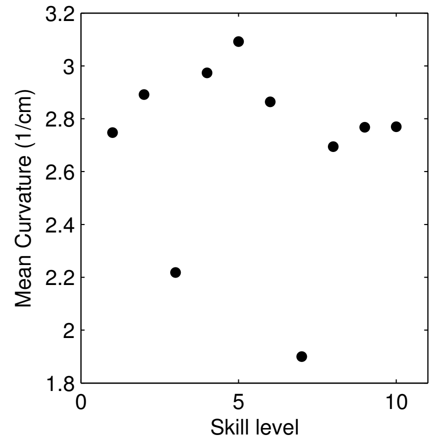

(b) Mean curvature of non-dominant hand for FLS task.

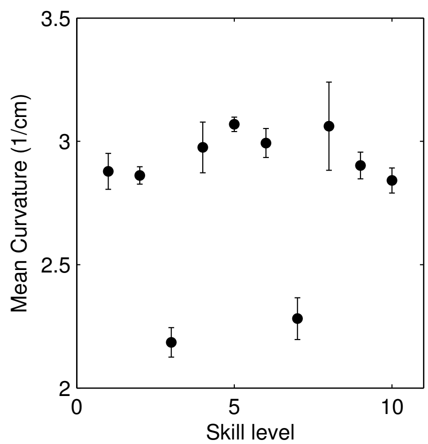

(c) Mean curvature of dominant hand for simple interrupted suturing.

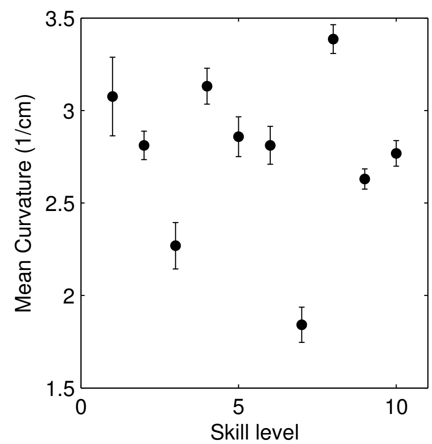

(d) Mean curvature of non-dominant hand for simple interrupted suture.

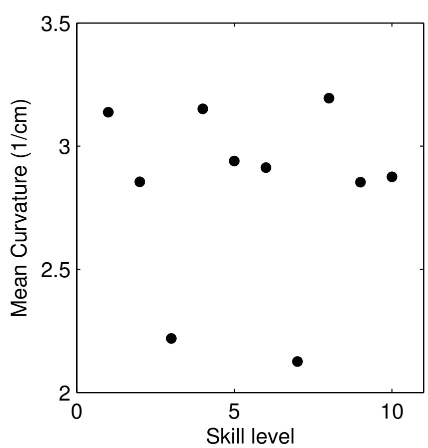

(e) Mean curvature of dominant hand for continuous running suture task.

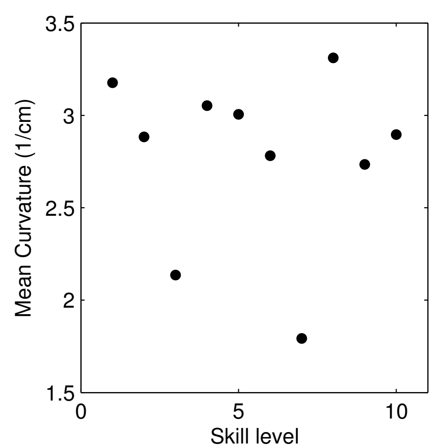

(f) Mean curvature of non-dominant hand for continuous running suture task.

Figure 5.4: Mean curvature for the performed tasks.

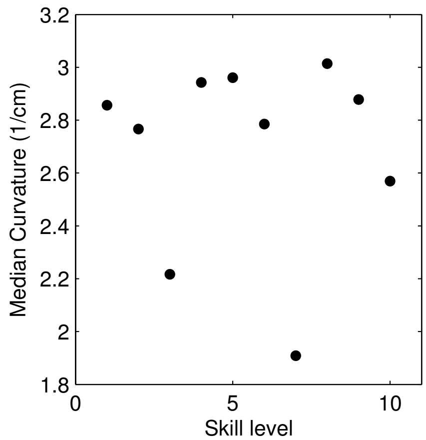

(a) Median curvature of dominant hand for FLS task.

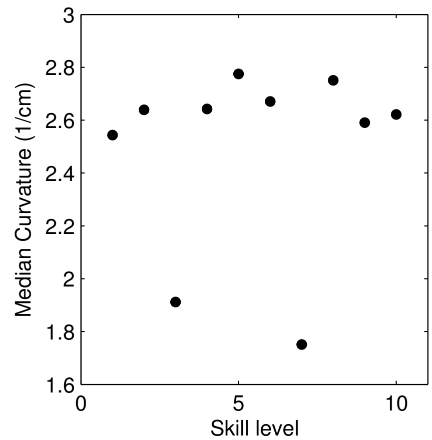

(b) Median curvature of non-dominant hand for FLS task.

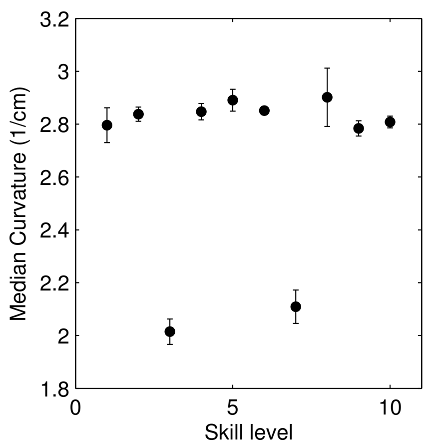

(c) Median curvature of dominant hand for simple interrupted suturing.

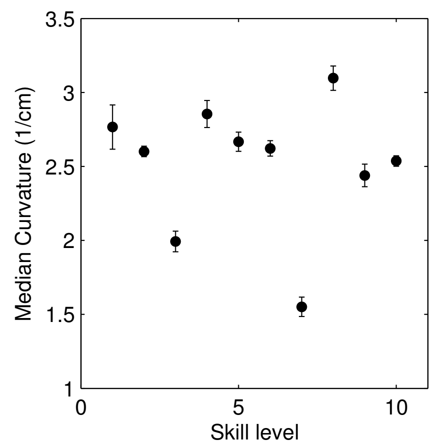

(d) Median curvature of non-dominant hand for simple interrupted suture.

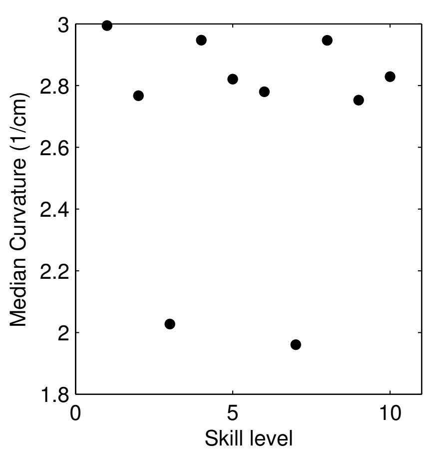

(e) Median curvature of dominant hand for continuous running suture task.

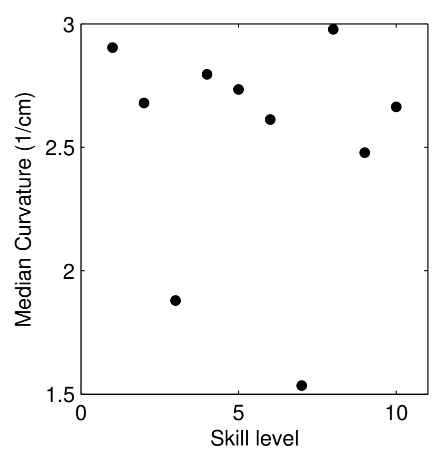

(f) Median curvature of non-dominant hand for continuous running suture task.

Figure 5.5: Median curvature for the performed tasks.

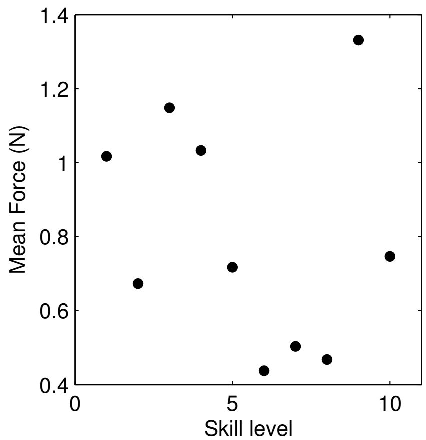

(a) Mean absolute force of dominant hand for FLS task.

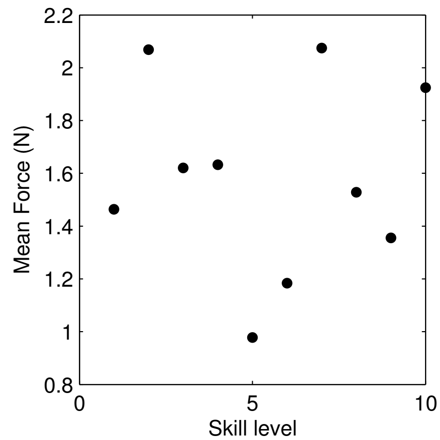

(b) Mean absolute force of non-dominant hand for FLS task.

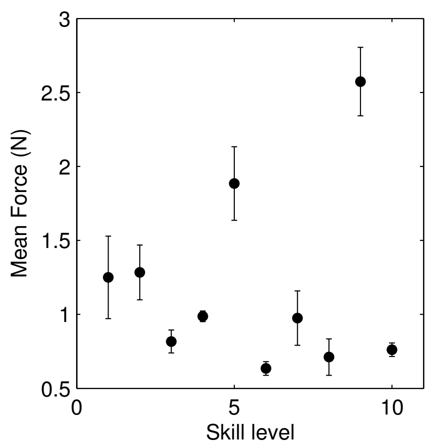

(c) Mean absolute force of dominant hand for simple interrupted suturing.

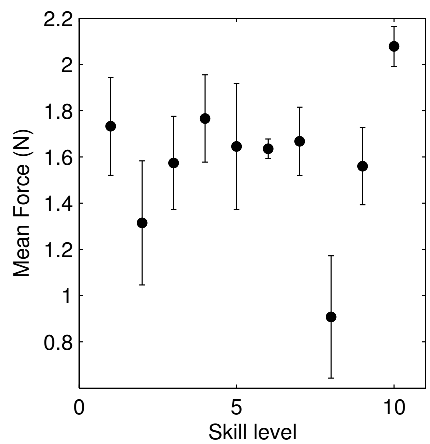

(d) Mean absolute force of non-dominant hand for simple interrupted suture.

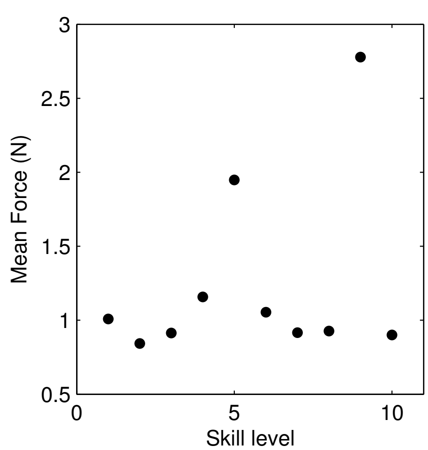

(e) Mean absolute force of dominant hand for continuous running suture task.

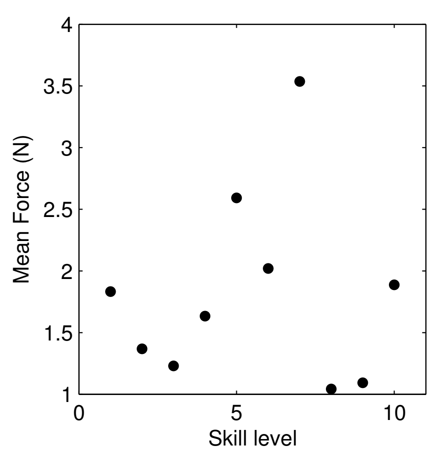

(f) Mean absolute force of non-dominant hand for continuous running suture task.

Figure 5.6: Mean absolute force for the performed tasks.

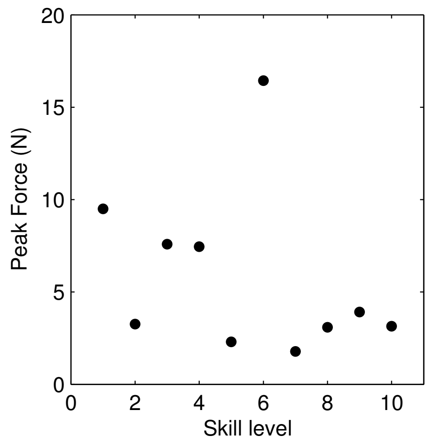

(a) Peak absolute force of dominant hand for FLS task.

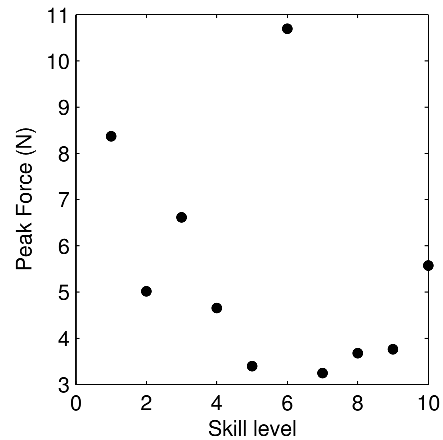

(b) Peak absolute force of non-dominant hand for FLS task.

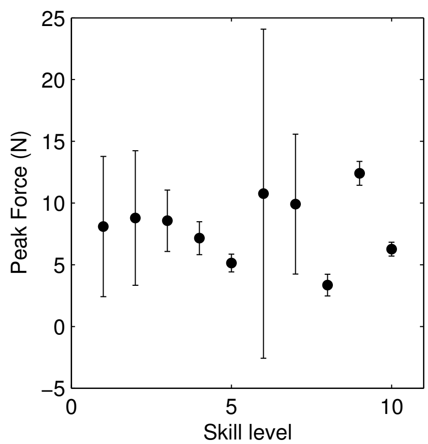

(c) Peak absolute force of dominant hand for simple interrupted suturing.

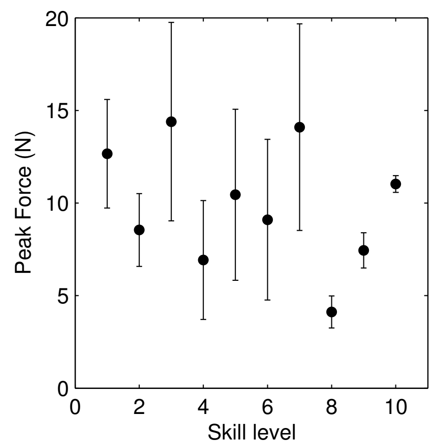

(d) Peak absolute force of non-dominant hand for simple interrupted suture.

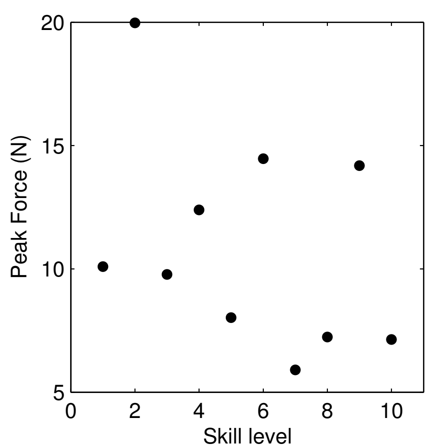

(e) Peak absolute force of dominant hand for continuous running suture task.

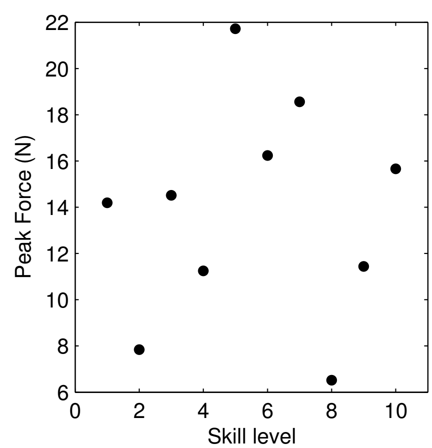

(f) Peak absolute force of non-dominant hand for continuous running suture task.

Figure 5.7: Peak absolute force for the performed tasks.

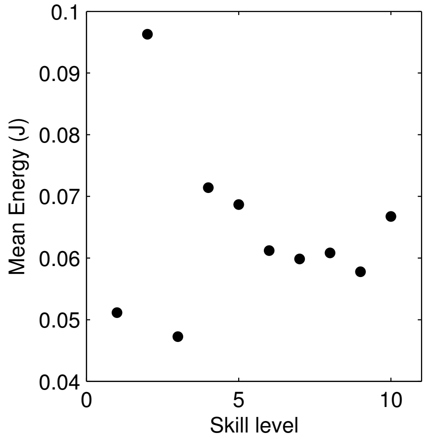

(a) Mean energy of dominant hand for FLS task.

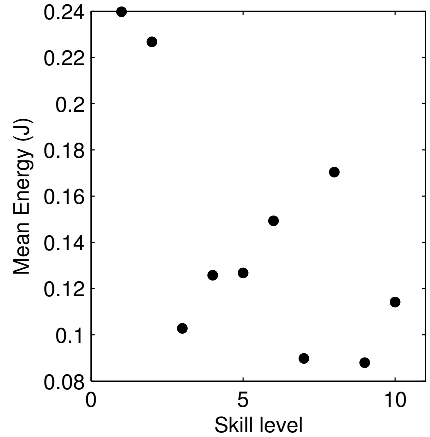

(b) Mean energy of non-dominant hand for FLS task.

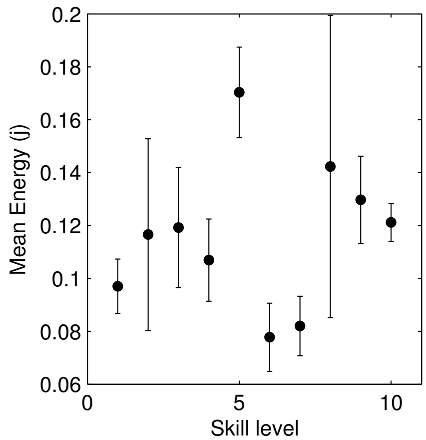

(c) Mean energy of dominant hand for simple interrupted suturing.

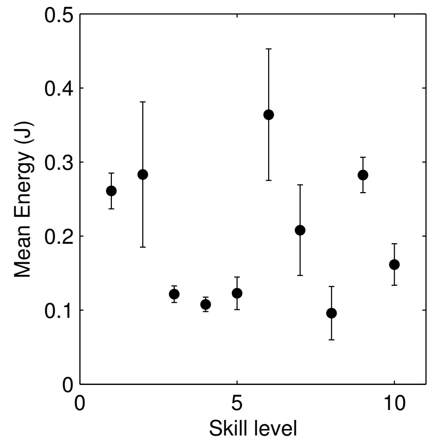

(d) Mean energy of non-dominant hand for simple interrupted suture.

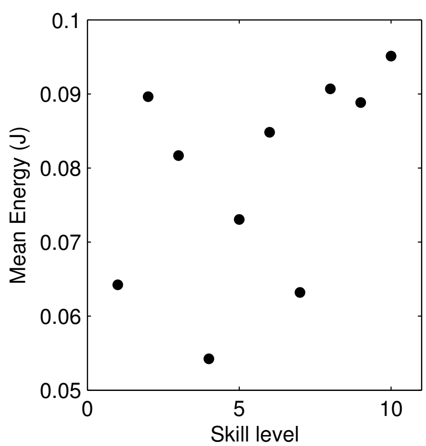

(e) Mean energy of dominant hand for continuous running suture task.

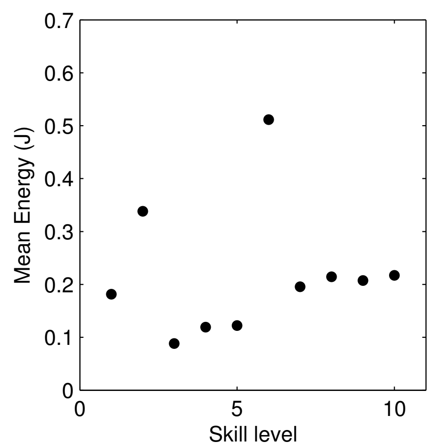

(f) Mean energy of non-dominant hand for continuous running suture task.

Figure 5.8: Mean energy for the performed tasks.

5.3 Local Analysis

Local analysis was performed on the simple interrupted sutures using both curvature and energy signals. The analysis measured how each surgeme was executed by the participant. This method took advantage of the fact that experts are more consistent and perform their movements more reliably. Currently, the surgemes are isolated using a manual segmentation process, which does remove some objectivity. However, other researchers are tackling the problem of automatic segmentation which will eliminate all subjective input.

5.3.1 Local Curvature

The curvature of the trajectories contains information that can be used to measure the similarity between two gestures. The similarity between trajectories was measured using a cross correlation operation on the curvature signals of those trajectories. The peak of the cross correlation was compared to a noise model which is described below to determine its significance. All four scales, described in Section 3.6.1 were analyzed empirically, and Scale 3 provided the most consistent results. Scales 1 and 2 typically contained many small spikes that did not represent the true movements of the surgeon. Scale 4 oversimplified the data and removed some of the useful signal. Only the results from Scale 3 are presented here.

Noise Model

Significance of the cross correlation operation was determined by comparing the cross correlation to a noise model. The noise model represents the cross correlation value that one might get when correlating two gestures that are unrelated. This model provides a baseline to compare other correlation values and test for their significance. If the cross correlation values for two gestures is higher than most that are generated by random correlations, then they can be said to be similar.

The noise model is a set of cross-correlation values of random segments generated using a bootstrapping technique. Ten thousand cross correlation operations were performed on pairs of random segments. Each segment of the pair could be from a different participant, or the same participant, and the only restriction on the pairs of segments was that they be from different surgemes. This ensured that the noise model represented the cross correlation of unrelated motions.

The set of cross correlation peaks is plotted in a histogram (Figure 5.9) that shows an approximate Gaussian distribution centered around 0. The standard deviation of the model is 0.29, and 95% of the values fall within -0.58 to 0.58. Any cross correlations larger than 0.58 were considered to be significant.

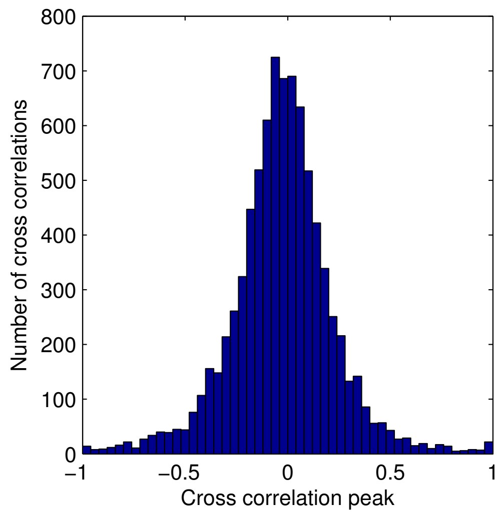

Figure 5.9: Histogram of curvature noise model calculated from Scale 3.

Curvature Correlation

Similarity between two segments is computed by calculating the peak of the normalized cross correlation between the curvature signals (κ_a, κ_b) of the gestures. The shorter of the two signals is padded with zeros so that both signals have the same length N. The curvature correlation value is calculated as

$$\rho_\kappa = \max_{s=-0.9\cdot N}^{0.9\cdot N} \left(\frac{1}{N-1} \cdot \sum_{i=1}^{N} \frac{(\kappa_a(i) - \bar{\kappa_a}) \cdot (\kappa_b(i+s) - \bar{\kappa_b})}{\sigma_{\kappa a} \cdot \sigma_{\kappa b}} \right) . \qquad (5.2)$$

Outliers in the resulting noise model were generated when very small portions of the two signals were used (e.g, less than ten samples). A Winsorizing technique eliminated these outliers by ignoring any cross correlation peaks that occurred within

10% of either end of the signal. If the Winsorizing technique is not used, small segments of the signal (two samples, for instance) could correlate highly even when the gestures are very dissimilar. This outlier elimination does not reduce the correlations of gestures that are truly similar, as the peaks are near the center of the cross-correlation signal. This is because the center of the cross correlation signal is the value that results when the two gestures are correlated without any offset. The threshold of 10% was chosen empirically after constructing a noise model with increasing thresholds until the noise model was centered around 0. The value of 0.9 in the calculation represents the 90% of the signal that is considered after the Winsorizing process. For all indices outside the range of [0, N], the curvature value is considered to be 0. That is, for $i < 0$ or $i > N$, $\kappa_a(i) = 0$, and $\kappa_b(i) = 0$.

The cross correlation process for computing gesture similarity is illustrated in Figure 5.10. The two signals to be correlated are shown in Figure 5.10a and Figure 5.10d. The un-normalized cross correlation is shown in Figure 5.10b. After discarding the first 10% and the last 10% of this cross correlation signal, the index with the peak value is found, in this case it is around sample index 175. This index gives the optimal alignment of the two signals, shown in Figures 5.10c and 5.10e.

Segments that are simple and performed quite similarly have highly correlated curvature signals such as the left instrument of the 'pull-through' segment performed by the top-ranked participant, shown in Figure 5.11a-e. As can be seen from the 3D plots (Figure 5.12a-e), the segment is very similar in the first four stitches, but the fifth stitch contains extra movements due to an error. This similarity and dissimilarity is reflected in the correlation values, with the correlation between all pairs of the first four stitches being significant ($\rho_\kappa > 0.58$), and all similarities between the first four stitches and the last stitch being insignificant ($\rho_\kappa < 0.58$).

The curvature correlation is also relatively low with novices whose movements are highly varied. The instrument in the left hand of the 'pull-through' segment is moved very differently by the participant ranked lowest (see Section 4.2.2 and Figure 5.13a-e). The length of these movements and the trajectories are quite different. These movements are of highly varying lengths, and the trajectories are quite different. Only two of the ten pairs of stitches have significant correlation, the rest are

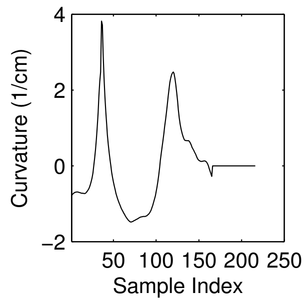

(a) Signal A

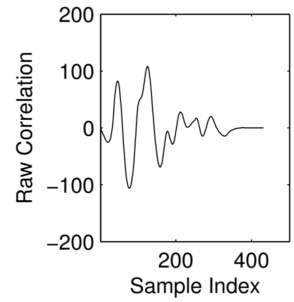

(b) Un-normalized cross correlation of signal A and signal B

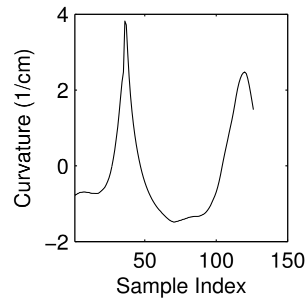

(c) Portion of signal A used in normalized correlation

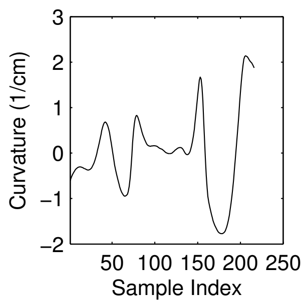

(d) Signal B

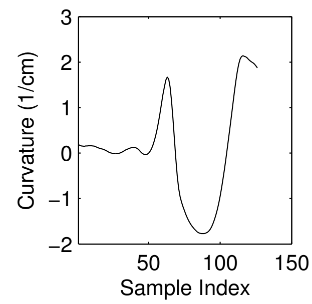

(e) Portion of signal B used in normalized correlation

Figure 5.10: Example curvature signals and the resulting cross correlation.

insignificant.

The use of curvature correlation as an indicator of skill is limited, however. There are several examples of novices performing movements that have high measures of similarity, such as the left hand of the insertion segment for the third lowest ranked participant. These trajectories are quite different but the resulting correlations are high, with eight of the ten pairs of stitches having significant correlations ($\rho_\kappa > 0.6$). A similar problem occurs with some expert movements, as in the left hand of the insertion segment of the top-ranked participant, shown in Figure 5.14a-e. Though these movements are very similar, the correlation values are low, with only one of the ten pairs of stitches having a significant correlation. These difficulties prevent a meaningful aggregation of data to use as a metric for surgical skill. No clear relationship is found between the mean of all of the self correlation values and the skill level, shown in Figure 5.15a-b.

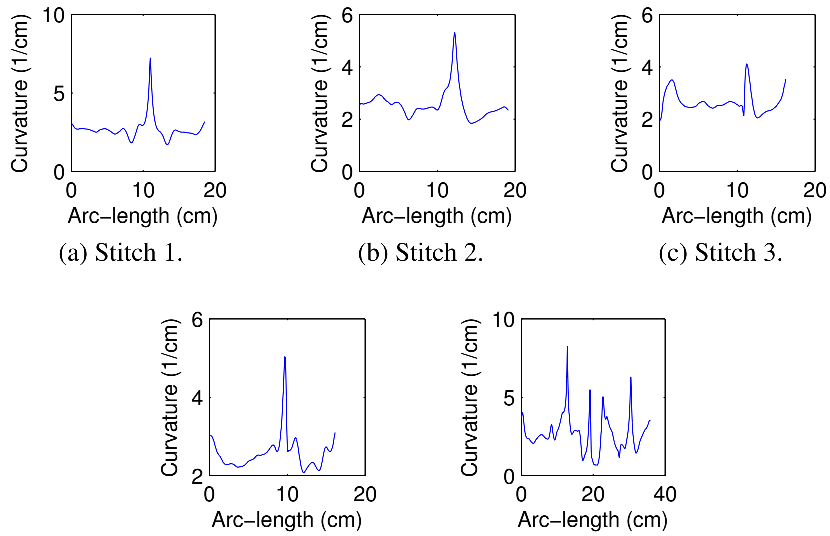

(a) Stitch 1. (b) Stitch 2. (c) Stitch 3.

(d) Stitch 4. (e) Stitch 5.

Figure 5.11: Curvature signal of the trajectory of the left instrument for the pull-through segment of the top-ranked participant.

Curvature Discussion

When analyzing simple gestures, curvature correlation is useful. Though neither is high after aggregation, the curvature correlations of the simpler movements of the left hand seemed to have a higher relationship to skill than the more complex movements of the right hand. This curvature-based approach seems more suited to dexemes rather than surgemes, but dexemes are not currently clearly defined making analysis difficult at this level. If a reliable segmentation process and suitable dexeme vocabulary is developed, curvature correlation could likely be used to construct a useful measure of similarity.

Curvature correlation is not effective for the longer motions characteristic of typical surgemes. The computation of the curvature is sensitive to noise, and unbounded. Complex gestures have increasingly complex curvature signatures that become more difficult to analyze and compare. Differences in signal length are largely unaccounted for, resulting in shorter signals that match well with a small window within a larger gesture.

The cross-correlation operation used to compute similarity between signals is likely too simple to provide a robust measure of skill. This comparison method is not robust to variations in the length of gesture. If a surgeon performs a gesture that is slightly longer or includes some idle movement, but is otherwise the same, it can severely reduce the correlation measure. Idle movement of the instrument can also produce delays in the signal which prevent useful correlation. More complex approaches, such as dynamic time warping, or comparing hidden Markov models generated from the curvature signals may provide a more robust estimator of skill from curvature.

Though the curvature correlation is not effective, the use of self-repetition seems to be a robust method of evaluating skill. By visual inspection, the trajectories of experts appear quite consistent. This visual inspection focussed mainly on the overall shape of the trajectories. Trajectories with clear changes in directions in the roughly same location were considered to be similar. Small deviations in the path were not considered to be significant. With more effective modelling techniques, this similarity could be quantified and more thoroughly analyzed. One benefit of using self-repetition is that the gestures need not be pre-defined, and no expert template is needed. This method would likely be limited to laboratory conditions, as there is too much natural variance in operating room conditions to allow for the same gestures to be performed consistently.

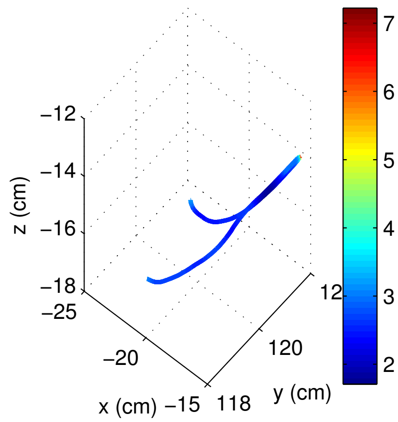

(a) Stitch 1.

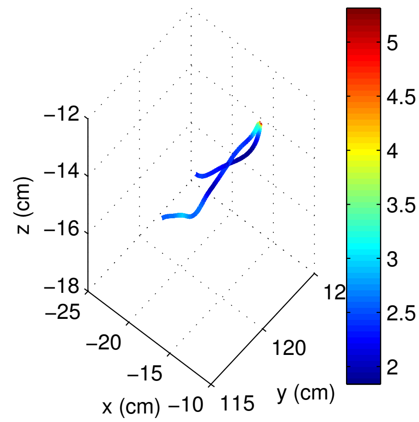

(b) Stitch 2.

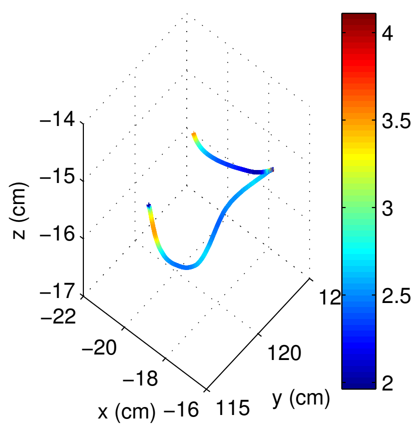

(c) Stitch 3.

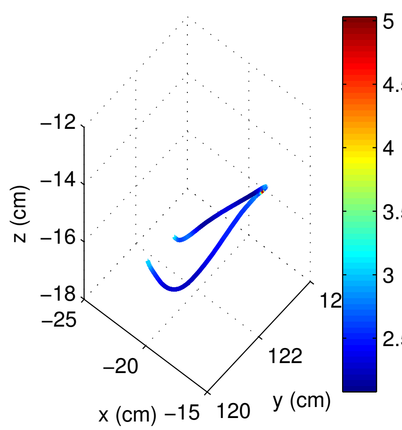

(d) Stitch 4.

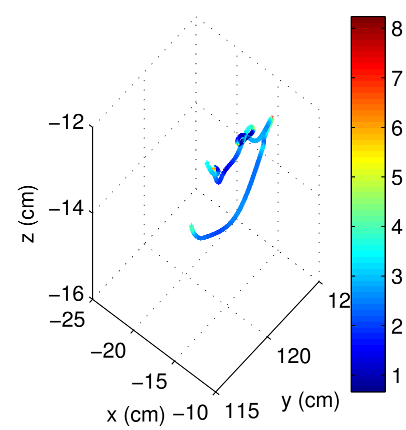

(e) Stitch 5.

Figure 5.12: Plots of the trajectory of the left instrument for the pull-through segment of the top-ranked participant with colour indicating curvature.

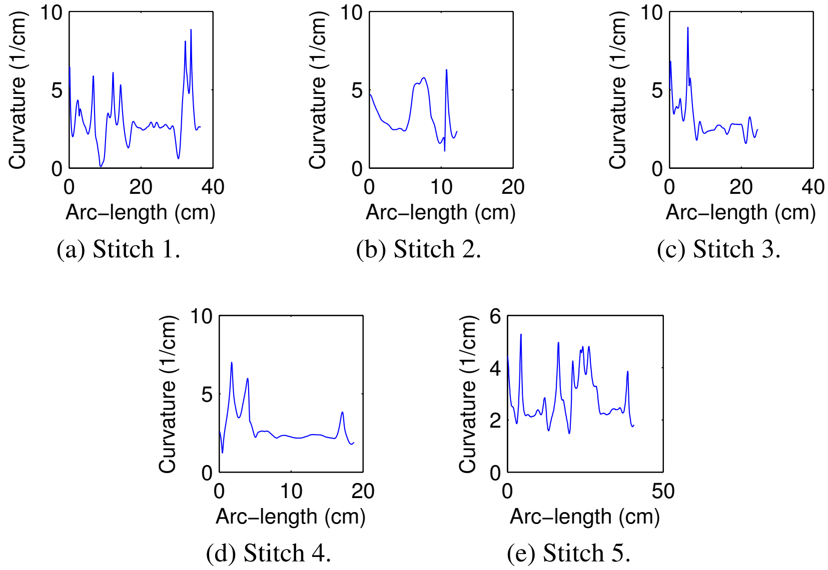

(a) Stitch 1. (b) Stitch 2. (c) Stitch 3. (d) Stitch 4. (e) Stitch 5.

Figure 5.13: Curvature signal of the trajectory of the left instrument for the pull-through segment of the lowest ranked participant.

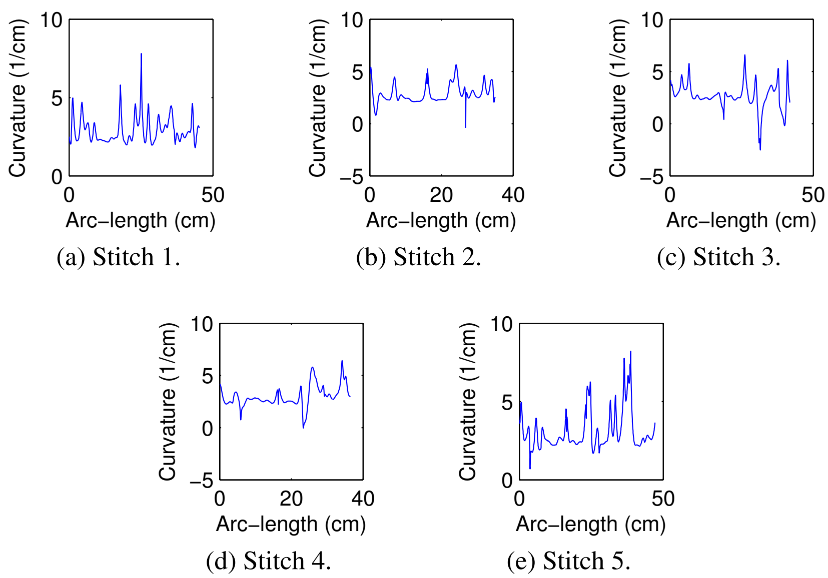

(a) Stitch 1. (b) Stitch 2. (c) Stitch 3. (d) Stitch 4. (e) Stitch 5.

Figure 5.14: Curvature signal of the trajectory of the left instrument for the insertion segment of the highest ranked participant.

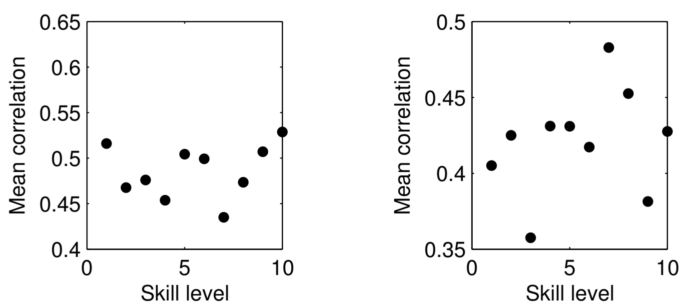

(a) Left hand

(b) Right hand

Figure 5.15: Mean curvature correlation for each participant.

5.3.2 Local Energy

Gesture similarity based on energy is computed in a similar way as the curvature signals. The energy signals are first resampled and mapped to the arc-length domain. Energy signals representing the same segment are then cross-correlated using the same Windsorised process as with the curvature signals. The peak of the resulting cross correlation of the energy is compared to the energy noise model to determine significance.

The noise model for energy was computed in much the same way as the noise model for curvature described in Section 5.3.1. Ten thousand randomly selected pairs were cross-correlated, and the same Winsorizing process was applied. The resulting model (Figure 5.16) has an approximate Gaussian distribution centered around 0, with a standard deviation of $\sigma = 0.27$. Cross correlation peaks above 0.54 are considered significant.

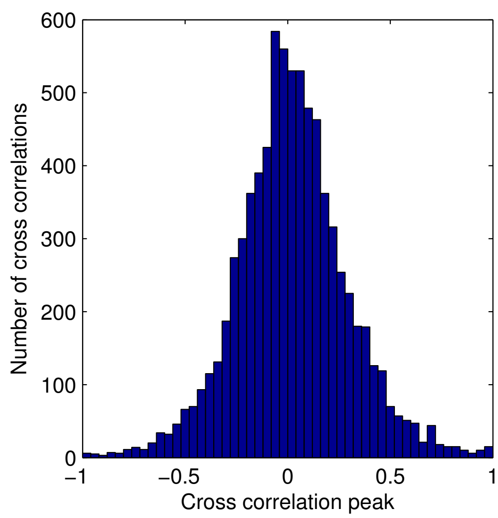

Figure 5.16: Histogram of energy noise model.

Energy Correlation

The energy signals were mapped into the arc-length domain to eliminate the time-dependence of the signal. The mapping was performed by assigning each arc-length index the energy value computed from the corresponding time frame using equation 3.1. No interpolation was used in this process.

The correlation value was computed as the peak of the normalized cross correlation between two energy signals, E_a and E_b.

$$\rho_E = \max_{s=-0.9\cdot N}^{0.9\cdot N} \left(\frac{1}{N-1} \cdot \sum_{i=1}^{N} \frac{(E_a(i) - \bar{E}_a) \cdot (E_b(i+s) - \bar{E}_b)}{\sigma_{Ea} \cdot \sigma_{Eb}} \right) . \tag{5.3}$$

Simple, similar gestures tend to correlate highly with this method, as was the case with curvature. This can be seen in the energy signal from the left hand of the 'double-loop' segment performed by the second-rank participant. As shown in Figure 5.17a-e, the trajectory and energy signal appear quite similar, and of the ten pairs of segments, eight correlate significantly ($\rho_E > 0.54$). The energy correlations also reflect dissimilarities in gestures (Figure 5.18). These trajectories and energy patterns are quite different and indicative of a novice. The energy correlation reflects this, with only two of the ten correlations being significant ($\rho_E > 0.54$).

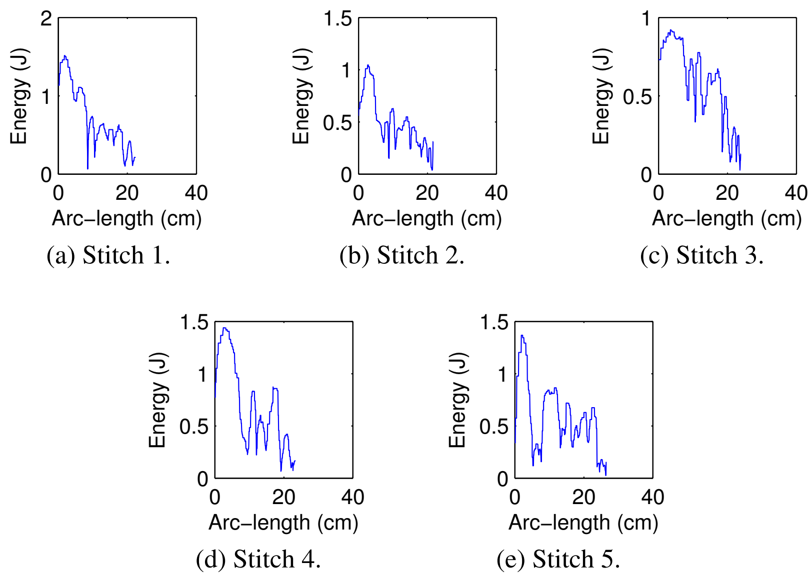

Figure 5.17: Energy signal of the trajectory of the left instrument for the 'double-loop' segment of the second-highest ranked participant.

Energy correlation seems more robust than curvature correlation when aggregating scores. While the mean ρ_E values of neither the left nor the right hand display a significant correlation with expert-assessed skill, there appears to be a trend with the left hand. As shown in Figure 5.19a, there is a strong positive correlation present if the outliers at rank 1 and 8 are ignored ($p < 0.01$). The equivalent correlation

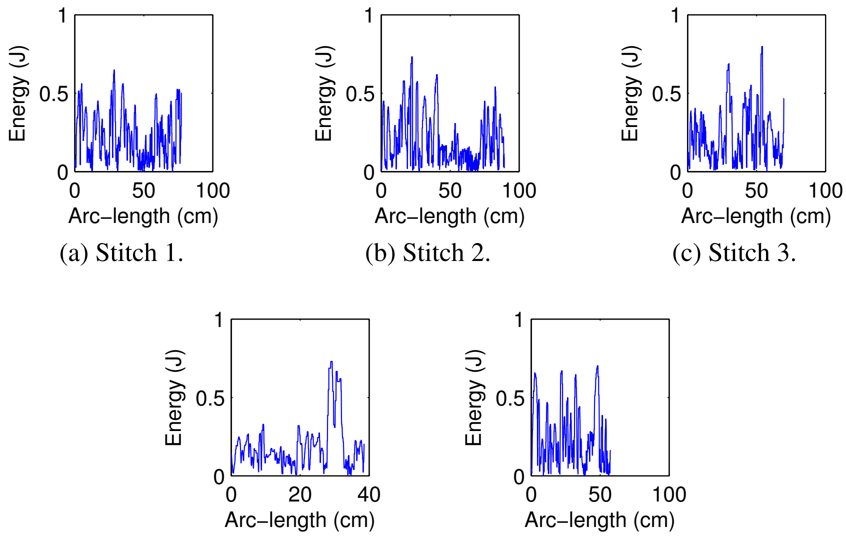

(a) Stitch 1. (b) Stitch 2. (c) Stitch 3.

(d) Stitch 4. (e) Stitch 5.

Figure 5.18: Energy signal of the trajectory of the left instrument for the ‘insertion’ segment of the third-worst ranked participant.

for the right hand does not show such a correlation (Figure 5.19b), likely due to the increased complexity of the movements of the right hand.

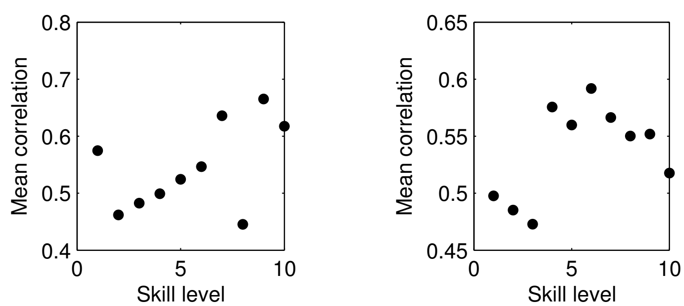

(a) Left hand (b) Right hand

Figure 5.19: Mean energy correlation for each participant.

Energy Discussion

Energy accounts for the forces that are applied, as well as the velocity of the instrument, which may result in the energy signal containing more useful information than the curvature signal. As with the curvature signals, the movements of the right hand are too complex to provide a meaningful measure. Again, the use of similarity measures that are more sophisticated than cross correlation will likely produce a stronger relationship between skill and energy signatures. By visual inspection, the energy correlation seems to support the use of self-repetition as an indicator of skill. The patterns of energy that are applied appear very similar, and more sophisticated techniques will likely produce a clear differentiation between the signals of an expert and those of a novice.

Chapter 6

Conclusions and Future Work

6.1 Conclusions

Automated evaluation of surgical skill removes the subjectivity and variability from current expert-based evaluation methods. Current methods of automated evaluation are not yet able to replace the expert evaluator due to the equipment needed and a lack of adequate skill metrics. Once refined, these methods will be able to provide feedback to trainees throughout their training program and evaluate the capabilities of trainees before they enter the operating room.

A system was designed that is capable of recording a wide range of data from participants performing laparoscopic tasks on a training box. The position and orientation of the instrument, and the kinematic structure of the participant's upper body were recorded using an optical motion captured device. Force and torque sensors placed on a pair of laparoscopic needle drivers record the dynamics of the participant's movements. Two video streams capture the view from the laparoscopic camera, as well as a birds-eye view of the participant performing the tasks. All data was synchronized and digitally stored for offline processing.

Empirical studies were conducted using the developed system. Participants performed a number of laparoscopic tasks while their movements were recorded. The study included a number of tasks that require different skill levels to be completed. The participants represented a broad range of skill, from first year residents to expert surgeons. This study provided a basis to study how the movements of surgeons differ with expertise.

Two global measures were developed. The global measure of total energy was found to be a useful indicator of skill, and appears to be complimentary to other measures of motion quantity. The mean and peak applied energy was not found to be significantly related to surgical, and illustrated the difficulty in using global measures to assess quality of movements.

The local analyses were performed using the curvature of the signal and the energy signature. While neither of these methods were able to clearly distinguish between novice and expert, they do show promise. Both methods showed a high correlation with surgical skill with simple gestures. By segmenting the gestures at the dexeme level, rather than the surgeme level it is likely that these methods will prove very effective.

6.2 Future Work

Developing a segmentation process that operates at the dexeme level would be very beneficial to surgical skill analysis. This would involve analyzing the various movements that surgeons use across different tasks and with different tools. From this, a complete vocabulary of dexemes could be developed. Once this vocabulary was in place, an automated segmentation process could be developed that would remove all subjective input to surgical skill evaluation.

More work can be done analyzing the orientation of the instrument as well. Global measures, such as total angular rotation, and average rotational velocity can be computed and analyzed for a relationship to surgical skill. A local analysis on the orientation can be performed as well in a similar manner to the curvature analysis.

Bibliography

[1] 3D-Med. TRLCD07 3-Dmed standard MITS with joystick SimScope description. http://www.3-dmed.com/TRLCD07__3-Dmed_Standard_MITS_with_Joystick_SimScope_Description.html, 2010.

[2] Motion Analysis. Motion analysis corporation, the motion capture leader. http://www.motionanalysis.com/, 2010.

[3] ATI. ATI industrial automation: Robotic end effectors and automation tooling. http://www.ati-ia.com/, 2010.

[4] S. D. Bann, M. S. Khan, and A. W. Darzi. Measurement of surgical dexterity using motion analysis of simple bench tasks. *World Journal of Surgery*, 27(4):390–394, 2003.

[5] T. Blum, N. Padoy, H. Feuner, and N. Navab. Modeling and online recognition of surgical phases using hidden markov models. *Medical Image Computing and Computer-Assisted Intervention*, pages 627–635, 2008.

[6] Z. Boom-Saad, S. A. Langenecker, L. A. Bieliauskas, C. J. Graver, J. R. O'Neill, A. F. Caveney, L. J. Greenfield, and R. M. Minter. Surgeons outperform normative controls on neuropsychologic tests, but age-related decay of skills persists. *The American Journal of Surgery*, 195(2):205–209, 2008.

[7] L. Bouarfa, P. P. Jonker, and J. Dankelman. Surgical context discovery by monitoring low-level activities in the OR. In *MICCAI Workshop on Modeling and Monitoring of Computer Assisted Interventions*, 2009.

[8] L. Bouarfa, P.P. Jonker, and J. Dankelman. Discovery of high-level tasks in the operating room. *Journal of Biomedical Informatics*, In Press, Corrected Proof:–, 2010.

[9] J. D. Brown, J. Rosen, L. Chang, M. N. Sinanan, and B. Hannaford. Quantifying surgeon grasping mechanics in laparoscopy using the blue DRAGON system. *Studies in Health Technology and Informatics*, pages 34–36, 2004.

[10] S. N. Buzink, A. D. Koch, J. Heemskerk, S. M. B. I. Botden, R. H. M. Goossens, H. de Ridder, E. J. Schoon, and J. J. Jakimowicz. Acquiring basic endoscopy skills by training on the GI mentor II. *Surgical Endoscopy*, 21(11):1996–2003, 2007.

[11] C. Cao, C. MacKenzie, and S. Payandeh. Task and motion analyses in endoscopic surgery. In *Proceedings ASME Dynamic Systems and Control Division*, pages 583–590, 1996.

[12] M. K. Chmarra. How to objectively classify residents based on their psychomotor laparoscopic skills? *Minimally Invasive Therapy & Allied Technologies*, 19(2), 2010.

[13] M. K. Chmarra, N. H. Bakker, C. A. Grimbergen, and J. Dankelman. TrEndo, a device for tracking minimally invasive surgical instruments in training setups. *Sensors & Actuators: A. Physical*, 126(2):328–334, 2006.

[14] M. K. Chmarra, C. A. Grimbergen, and J. Dankelman. Systems for tracking minimally invasive surgical instruments. *Minimally Invasive Therapy & Allied Technologies*, 16(6):328–340, 2007.

[15] M. K. Chmarra, S. Klein, J. C. F. de Winter, F. W. Jansen, and J. Dankelman. Objective classification of residents based on their psychomotor laparoscopic skills. *Surgical Endoscopy*, 24(5):1031–1039, 2010.

[16] M. K. Chmarra, W. Kolkman, F. W. Jansen, C. A. Grimbergen, and J. Dankelman. The influence of experience and camera holding on laparoscopic instrument movements measured with the TrEndo tracking system. *Surgical Endoscopy*, 21(11):2069–2075, 2007.

[17] S. Cotin, N. Stylopoulos, M. Ottensmeyer, P. Neumann, D. Rattner, and S. Dawson. Metrics for laparoscopic skills trainers: the weakest link! *Medical Image Computing and Computer-Assisted Intervention*, pages 35–43, 2002.

[18] S. M. Cristancho, A. J. Hodgson, O. N. M. Panton, A. Meneghetti, G. Warnock, and K. Qayumi. Intraoperative monitoring of laparoscopic skill development based on quantitative measures. *Surgical endoscopy*, 23(10):2181–2190, 2009.

[19] V. Datta, A. Chang, S. Mackay, and A. Darzi. The relationship between motion analysis and surgical technical assessments. *American Journal of Surgery*, 184(1):70, 2002.

[20] V. Datta, S. Mackay, M. Mandalia, and A. Darzi. The use of electromagnetic motion tracking analysis to objectively measure open surgical skill in the laboratory-based model. *Journal of the American College of Surgeons*, 193(5):479, 2001.

[21] M. D. Derossis, M. Anna, M. D. Fried, M. Gerald, M. Abrahamowicz PhD, M. D. Sigman, H. Harvey, M. D. Barkun, S. Jeffrey, and M. D. Meakins. Development of a model for training and evaluation of laparoscopic skills. *The American Journal of Surgery*, 175(6):482–487, 1998.

[22] DivX. DivX - download DivX software & find devices that play DivX video | DivX.com. http://www.divx.com/en/mac, 2010.

[23] A. Dosis, R. Aggarwal, F. Bello, K. Moorthy, Y. Munz, D. Gillies, and A. Darzi. Synchronized video and motion analysis for the assessment of procedures in the operating theater. *Archives of Surgery*, 140(3):293, 2005.

[24] P. Dubois, Q. Thommen, and A. C. Jambon. In vivo measurement of surgical gestures. *IEEE Transactions on Biomedical Engineering*, 49(1):49–54, 2002.

[25] A. Dubrowski, R. Sidhu, J. Park, and H. Carnahan. Quantification of motion characteristics and forces applied to tissues during suturing. *The American Journal of Surgery*, 190(1):131–136, 2005.

[26] T. A. Emam, G. B. Hanna, C. Kimber, and A. Cuschieri. Differences between experts and trainees in the motion pattern of the dominant upper limb during intracorporeal endoscopic knotting. *Digestive surgery*, 17(2):120, 2000.

[27] T. A. Emam, G. B. Hanna, C. Kimber, P. Dunkley, and A. Cuschieri. Effect of intracorporeal-extracorporeal instrument length ratio on endoscopic task performance and surgeon movements. *Archives of Surgery*, 135(1):62, 2000.

[28] C. Feng, H. Haniffa, J. Rozenblit, J. Peng, A. Hamilton, and M. Salkini. Surgical training and performance assessment using a motion tracking system. In *2nd European Modeling and Simulation Symposium. EMSS 2006*, pages 647–652, 2006.

[29] E. D. Grober, M. Roberts, E. J. Shin, M. Mahdi, and V. Bacal. Intraoperative assessment of technical skills on live patients using economy of hand motion: establishing learning curves of surgical competence. *The American Journal of Surgery*, 199(1):81–85, 2010.

[30] S. Gunther, J. Rosen, B. Hannaford, and M. Sinanan. The red DRAGON: a multi-modality system for simulation and training in minimally invasive surgery. *Studies in health technology and informatics*, 125:149, 2007.

[31] H. Hwang, J. Lim, C. Kinnaird, A. G. Nagy, O. N. M. Panton, A. J. Hodgson, and K. A. Qayumi. Correlating motor performance with surgical error in laparoscopic cholecystectomy. *Surgical Endoscopy*, 20(4):651–655, 2006.

[32] T. N. Judkins, D. Oleynikov, and N. Stergiou. Objective evaluation of expert and novice performance during robotic surgical training tasks. *Surgical Endoscopy*, 23(3):590–597, 2009.

[33] P. S. Kundhal and T. P. Grantcharov. Psychomotor performance measured in a virtual environment correlates with technical skills in the operating room. *Surgical Endoscopy*, 23(3):645–649, 2009.

[34] P. Lamata, E. J. Gomez, F. L. Hernandez, A. O. Pastor, F. M. Sanchez-Margallo, and F. del Pozo Guerrero. Understanding perceptual boundaries in laparoscopic surgery. *IEEE Transactions on Biomedical Engineering*, 55(3):866–873, 2008.

[35] LapSim. PRODUCTS - surgical science. http://www.surgical-science.com/productsmain/, 2010.

[36] J. J. H. Leong, M. Nicolaou, L. Atallah, G. P. Mylonas, A. W. Darzi, and G. Z. Yang. HMM assessment of quality of movement trajectory in laparoscopic surgery. *Computer Aided Surgery*, 12(6):335–346, 2007.

[37] H. C. Lin, I. Shafran, T. E. Murphy, A. M. Okamura, D. D. Yuh, and G. D. Hager. Automatic detection and segmentation of robot-assisted surgical motions. *Lecture Notes in Computer Science*, 3749:802, 2005.

[38] LiveInCode. LiveInCode. http://liveincode.rm.pp.ru/, 2010.

[39] Logitech. QuickCam orbit MP. http://www.logitech.com/en-us/435/245, 2010.

[40] J. A. Martin, G. Regehr, R. Reznick, H. MacRae, J. Murnaghan, C. Hutchison, and M. Brown. Objective structured assessment of technical skill (OSATS) for surgical residents. *British Journal of Surgery*, 84(2), 1997.

[41] MATLAB. The MathWorks - MATLAB and simulink for technical computing. http://www.mathworks.com/, 2010.

[42] R. Moreau, V. Ochoa, M. T. Pham, P. Boulanger, T. Redarce, and O. Dupuis. Evaluation of obstetric gestures: An approach based on the curvature of 3-D positions. In *29th Annual International Conference of the IEEE Engineering in Medicine and Biology Society, 2007. EMBS 2007*, pages 3634–3637, 2007.

[43] NationalInstruments. National instruments - test and measurement. http://www.ni.com/, 2010.

[44] J. A. Oostema, M. P. Abdel, and J. C. Gould. Time-efficient laparoscopic skills assessment using an augmented-reality simulator. *Surgical Endoscopy*, 22(12):2621–2624, 2008.

[45] OpenCV. Welcome - OpenCV wiki. http://opencv.willowgarage.com/wiki/, 2010.

[46] OptoTrak. Optotrak certus motion capture system - Research-Grade motion capture system for life sciences applications | NDI. http://www.ndigital.com/lifesciences/certus-motioncapturesystem.php, 2010.

[47] N. Padoy, T. Blum, I. Essa, H. Feussner, M. O. Berger, and N. Navab. A boosted segmentation method for surgical workflow analysis. In *Medical Image Computing and Computer-Assisted Intervention*, pages 102–109. Springer-Verlag, 2007.

[48] N. Padoy, T. Blum, H. Feussner, M. O. Berger, and N. Navab. On-line recognition of surgical activity for monitoring in the operating room. In *Procs of the 20th Conference on Innovative Applications of Artificial Intelligence (IAAI-08)*, 2008.

[49] Purdue Pegboard. Purdue pegboard test | human evaluation from lafayette instrument company. http://www.lafayetteevaluation.com/product_detail.asp?ItemID=159, 2010.

[50] M. G. C. Pellen, L. F. Horgan, J. R. Barton, and S. E. Attwood. Construct validity of the ProMIS laparoscopic simulator. *Surgical Endoscopy*, 23(1):130–139, 2009.

[51] PTIPhoenix. PTI high performance Real-Time 3D motion capture for professionals. http://www.ptiphoenix.com/, 2010.

[52] RanDOT. Stereo fly and other StereoTests stereopsis, strabismus, and amblyopia testing. http://www.stereooptical.com/html/stereo-test.html, 2010.

[53] C. Reiley and G. Hager. Task versus subtask surgical skill evaluation of robotic minimally invasive surgery. *Medical Image Computing and Computer-Assisted Intervention*, pages 435–442, 2009.

[54] C. E. Reiley, H. C. Lin, B. Varadarajan, B. Vagvolgyi, S. Khudanpur, D. D. Yuh, and G. D. Hager. Automatic recognition of surgical motions using statistical modeling for capturing variability. *Studies in health technology and informatics*, 132:396, 2008.

[55] C. E. Reiley, H. C. Lin, D. D. Yuh, and G. D. Hager. Review of methods for objective surgical skill evaluation. *Surgical Endoscopy*, pages 1–11, 2009.

[56] C. Richards, J. Rosen, B. Hannaford, C. Pellegrini, and M. Sinanan. Skills evaluation in minimally invasive surgery using force/torque signatures. *Surgical Endoscopy*, 14(9):791–798, 2000.

[57] E. M. Ritter, T. W. Kindelan, C. Michael, E. A. Pimentel, and M. W. Bowyer. Concurrent validity of augmented reality metrics applied to the fundamentals of laparoscopic surgery (FLS). *Surgical Endoscopy*, 21(8):1441–1445, 2007.

[58] J. Rosen, J. D. Brown, L. Chang, M. Barreca, M. Sinanan, and B. Hannaford. The BlueDRAGON - a system for measuring the kinematics and the dynamics of minimally invasive surgical tools InVivo. In *IEEE International Conference on Robotics and Automation*, volume 2, pages 1876–1881, 2002.

[59] J. Rosen, J. D. Brown, L. Chang, M. N. Sinanan, and B. Hannaford. Generalized approach for modeling minimally invasive surgery as a stochastic process using a discrete markov model. *IEEE Transactions on Biomedical Engineering*, 53(3):399–413, 2006.

[60] J. Rosen, L. Chang, J. D. Brown, B. Hannaford, M. Sinanan, and R. Satava. Minimally invasive surgery task decomposition-etymology of endoscopic suturing. *Studies in Health Technology and Informatics*, pages 295–301, 2003.

[61] J. Rosen, M. MacFarlane, C. Richards, B. Hannaford, and M. Sinanan. Surgeon-tool force/torque signatures evaluation of surgical skills in minimally invasive surgery. *Medicine Meets Virtual Reality: The Convergence of Physical & Informational Technologies: Options for a New Era in Healthcare*, 62:290–296, 1999.

[62] J. Rosen, M. Solazzo, B. Hannaford, and M. Sinanan. Objective laparoscopic skills assessments of surgical residents using hidden markov models based on haptic information and tool/tissue interactions. *Studies in Health Technology and Informatics*, pages 417–423, 2001.

[63] J. Rosen, M. Solazzo, B. Hannaford, and M. Sinanan. Task decomposition of laparoscopic surgery for objective evaluation of surgical residents' learning curve using hidden markov model. *Computer Aided Surgery*, 7(1):49–61, 2002.

[64] G. M. Saleh, Y. Voyazis, J. Hance, J. Ratnasothy, and A. Darzi. Evaluating surgical dexterity during corneal suturing. *Archives of Ophthalmology*, 124(9):1263, 2006.

[65] S. Sinigaglia, G. Megali, O. Tonet, A. Pietrabissa, and P. Dario. Defining metrics for objective evaluation of surgical performances in laparoscopic training. In *International Congress Series*, volume 1281, pages 509–514. Elsevier, 2005.

[66] Inuitive Surgical. Intuitive surgical, inc. - da vinci surgical system. http://www.intuitivesurgical.com/index.aspx, 2010.

[67] Symbionix. LAP mentor laparoscopic surgery simulator for general surgery, gynecology and urology. http://www.simbionix.com/LAP_Mentor.html, 2010.

[68] K. Tanoue, S. Yamaguchi, K. Konishi, T. Yasunaga, D. Yoshida, N. Kinjo, K. Kobayashi, S. Ieiri, K. Okazaki, and H. Nakashima. Construct validity for eyehand coordination skill on a virtual reality laparoscopic surgical simulator. *Surgical Endoscopy*, 21(12):2253–2257, 2007.

[69] A. L. Trejos, R. V. Patel, M. D. Naish, and C. M. Schlachta. Design of a sensorized instrument for skills assessment and training in minimally invasive surgery. In *2nd IEEE RAS & EMBS International Conference on Biomedical Robotics and Biomechatronics, 2008. BioRob 2008*, pages 965–970, 2008.

[70] K. W. van Dongen, E. Tournoij, D. C. van der Zee, M. P. Schijven, and IAMJ Broeders. Construct validity of the LapSim: can the LapSim virtual reality simulator distinguish between novices and experts? *Surgical Endoscopy*, 21(8):1413–1417, 2007.

[71] M. C. Vassiliou, L. S. Feldman, C. G. Andrew, S. Bergman, K. Leffondr, D. Stanbridge, and G. M. Fried. A global assessment tool for evaluation of intraoperative laparoscopic skills. *The American Journal of Surgery*, 190(1):107–113, 2005.

[72] E. G. G. Verdaasdonk, L. P. S. Stassen, M. P. Schijven, and J. Dankelman. Construct validity and assessment of the learning curve for the SIMENDO endoscopic simulator. *Surgical Endoscopy*, 21(8):1406–1412, 2007.

[73] Vicon. Motion capture systems from vicon. http://www.vicon.com/, 2010.

[74] J. F. Waljee, L. J. Greenfield, J. B. Dimick, and J. D. Birkmeyer. Surgeon age and operative mortality in the united states. *Annals of surgery*, 244(3):353, 2006.

[75] G. Xeroulis, A. Dubrowski, and K. Leslie. Simulation in laparoscopic surgery: a concurrent validity study for FLS. *Surgical Endoscopy*, 23(1):161–165, 2009.

Appendix A

Pre-trial Questionnaire

Age:

Gender:

Male / Female

Dominant Hand:

Left / Right

Level:

None	Med Student	R1	R2	R3	R4	R5	Fellow	“Expert”

Do you have normal, or corrected to normal vision?

Yes / No

If you are a med student, do you have an interest in surgery?

Yes / No

How would you rate your laparoscopic suturing skills?

1	2	3	4	5
No Experience	I have practiced on endo-trainers;	I have learned the basic skills I am confident with my skills; ready to suture in the OR on patients	Experience performing full operations	Expert surgeon

How would you rate your skills in open surgical procedures?

1	2	3	4	5
No Experience	I have practiced on synthetic tissue; I have learned the basic skills	I am confident with my skills; ready to suture in the OR on patients	Experience performing full operations	Expert surgeon

Have you performed a laparoscopic cholecystectomy?

Approximately how many operations:

Have you performed a laparoscopic fundoplication?

Approximately how many operations:

Do you regularly play video games, or perform tasks involving fine motor skills or hand eye co-ordination (repair small machines, assemble models, etc.)? Please describe.

How many hours of sleep have you missed in the last week (i.e. due to call commitments, travel, illness)?

How many caffeinated drinks (coffee, tea, energy drinks) have you had in the last 24 hours?

When was the last time you performed, or practiced, hands-on laparoscopy (on synthetic or live tissue) (how many days ago)?

Appendix B

Post-trial Questionnaire

How would you rate your performance today?

1	2	3	4	5
Poor performance	Below average	Average performance	Above average performance	Very good performance